NATURAL CONVECTION INVESTIGATION AND PERFORMANCE ENHANCEMENT OF SOLAR CHIMNEY POWER PLANT

Ibrahim Shikh HASAN

2022
MASTER THESIS
MECHANICAL ENGINEERING

Thesis Advisor
Prof. Dr. Kamil ARSLAN

NATURAL CONVECTION INVESTIGATION AND PERFORMANCE ENHANCEMENT OF SOLAR CHIMNEY POWER PLANT

Ibrahim Shikh HASAN

T.C.
Karabük University
Institute of Graduate Programs
Department of Mechanical Engineering
Prepared as
Master Thesis

Thesis Advisor
Prof. Dr. Kamil ARSLAN

KARABÜK
April 2022

I certify that in my opinion the thesis submitted by IBRAHIM SHIKH HASAN titled "NATURAL CONVECTION INVESTIGATION AND PERFORMANCE ENHANCEMENT OF SOLAR CHIMNEY POWER PLANT" is fully adequate in scope and in quality as a thesis for the degree of Master of Science.

Prof. Dr. Kamil ARSLAN .....
Thesis Advisor, Department of Mechanical Engineering

This thesis is accepted by the examining committee with a unanimous vote in the Department of Mechanical Engineering as a Master of Science thesis. January 24, 2022

Examining Committee Members (Institutions)		Signature
Chairman	: Assoc. Prof. Dr. Engin GEDİK (KBU)	.....
Member	: Prof. Dr. Kamil ARSLAN (KBU)	.....
Member	: Assist. Prof. Dr. Hüseyin KAYA (BU)	.....

The degree of Master of Science by the thesis submitted is approved by the Administrative Board of the Institute of Graduate Programs, Karabük University.

Prof. Dr. Hasan SOLMAZ .....
Director of the Institute of Graduate Programs

"I declare that all the information within this thesis has been gathered and presented in accordance with academic regulations and ethical principles and I have according to the requirements of these regulations and principles cited all those which do not originate in this work as well."

Ibrahim Shikh HASAN

ABSTRACT

M. Sc. Thesis

NATURAL CONVECTION INVESTIGATION AND PERFORMANCE ENHANCEMENT OF SOLAR CHIMNEY POWER PLANT

Ibrahim Shikh HASAN

Karabük University
Institute of Graduate Programs
The Department of Mechanical Engineering

Thesis Advisor:
Prof. Dr. Kamil ARSLAN
April 2022, 64 pages

In this study, solar chimney power plant is numerically investigated by using *3D* model, standard *k-ε* model as fully turbulent flow, and Discrete Ordinates model (*DO*) as solar calculations. This study is based on Manzanares pilot data which are 194.6 *m* chimney elevation, 1.85 *m* collector height, 122 *m* collector radius, 5.08 *m* chimney radius 20 *˚C* plant mean temperature, and 15 *m/s* air velocity within the pilot to apply a fined collector as way of development.

To evaluate the new collector, a parametric study was carried out by varying number of fins between 25, 33 and 46; thickness of fins between 0.1, 0.25 and 0.5 *m*, and height of fins between 0.6, 0.925 and 1.2 *m*.

As a result, the new collector has been suggested to get the best outcomes. The dimensions are 46, 0.1 *m*, 1.2 *m* which are the number of fins, fin thickness, and fin

height, respectively. The plant efficiency, plant power outcome, Nusselt number, and Rayleigh number for optimum case are 1.674%, 700597 *W*, 1790.3, and 1.96E+14, respectively.

Key Words : Natural Convection, Solar Chimney, CFD, fined collector.
Science Code : 91441

ÖZET

Yüksek Lisans Tezi

GÜNEŞ BACA SANTRALİ DOĞAL KONVEKSYON ARAŞTIRMA VE PERFORMANS ARTIRMASI

Ibrahım Shıkh HASAN

Karabük Üniversitesi
Lisansüstü Eğitim Enstitüsü
Makine Mühendisliği Anabilim Dalı

Tez Danışmanı:
Prof. Dr. Kamil ARSLAN
Nisan 2022, 64 sayfa

Bu çalışmada, üç boyutlu tam türbülans akış şartlarında güneş bacası santrali sayısal olarak incelenmiştir. Çalışma, 194,6 *m* baca yüksekliği, 1,85 *m* kollektör yüksekliği, 122 *m* kollektör yarıçapı, 5,08 *m* baca yarıçapı 20 ^{o}C santral ortalama sıcaklığı ve 15 m/s hava hızını sunan sistem verilerine, kanatçıklı kolektör uygulayabilmek amacına dayanmaktadır.

Tez kapsamında kollektör içerisine kanatçık sayısı olarak 25, 33 ve 46; kanat kalınlığıolarak 0,1, 0,25 ve 0,5 *m*; ve kanat yüksekliği olarak ise 0,6, 0,925 ve 1,2 *m* olarak değişen kanatçık yapıları uygulanarak bir parametrik çalışma yapılmıştır.

Sonuç olarak, yeni kollektör için en iyi sonuçları elde etmek amacıyla optimum değerler elde edilmiştir. Optimum kanatçık sayısı, kanatçık kalınlığı ve kanatçık yüksekliğinin sırasıyla, 46, 0,1 *m* ve 1,2 *m* olduğu saptanmıştır. Ayrıca, optimum

verim, santral güç çıktısı, Nusselt sayısı ve Rayleigh sayısının ise sırasıyla, 1,674%, 700597 *W*, 1790,3 ve 1,96E+14 oldukları görülmüştür.

Anahtar Kelimeler **:** Güneş bacası santrali, CFD, Doğal konveksiyon.
Bilim Kodu **:** 91441

ACKNOWLEDGMENT

First of all, I would like to express my gratitude to my supervisor Prof. Dr. Kamil ARSLAN for his guidance and patience all these years and throughout my thesis study. I have experienced great academicall behavior under his supervision. Finally, I thank my family especially my parents from my heart for their support, patience, and generosity all the time.

CONTENTS

Page

Page

Page

LIST OF FIGURES

Page

Page

LIST OF TABLES

Page

SYMBOLS AND ABBREVIATIONS INDEX

SYMBOLS

ρ : density

ρ_∞ : the density of free stream

T : temperature

T_∞ : ambient or free-stream temperature

T_s : surface temperature

t : thickness

α : absorptivity

β : volume expansion coefficient

ε : emissivity

τ : transmissivity

v : kinematic viscosity

μ : dynamic viscosity

g : gravity

h : heat transfer coefficient

D : diameter

k. : conductivity

L_c : characteristic length

A_s : surface area

Nu : Nusselt number

Ra : Rayleigh number

Gr : Grashof number

G_k : generation of turbulence kinetic energy due to the mean velocity gradients

G_b : generation of turbulence kinetic energy due to buoyancy

Y_m : the contribution of the fluctuating dilatation in compressible turbulence to the overall dissipation rate

η : thermal efficiency

$\dot{W}_t$: turbine output power

$\dot{Q}_{in}$: total solar heat flux

I : solar flux

$\dot{m}$: mass flow rate

P : static pressure

V : velocity

$\bar{u}$: velocity on x

$\bar{v}$: velocity on y

Z : elevation

u : internal energy

$\bar{h}$: static enthalpy

$q_{net\ in}$: overall heat loss

R : collector radius

ΔT_{mean} : the temperature variance with the environment

$C_{1\epsilon}$, $C_{2\epsilon}$ $C_{3\epsilon}$, C and n: constants.

σ_k and σ_ϵ: turbulent Prandtl numbers.

S_k and S_ϵ: user-defined source terms

ABBREVIATIONS

SUT : Solar Upwind Tower

SCPP : Solar Chimney Power Plant

Ch/C : Nick Between Chimney and Collector

Ch/A : Nick Between Chimney and Absorber

PMC : Phase Change Materials

PART 1

INTRODUCTION

Nowadays power demand is significantly increased because of human rapid improvement and lifestyle. As a result, power is one of the main stones of the structure of the economy, authority, and future which encourages governments to get different resources like oil and coal, unfortunately, these and other resources harm humans or the environment plus they will finish soon. In light of that, the terms of renewable and clean energy appeared. Clean energy is a concept for energy that is friendly to the environment and does no harm to it and renewable is something that can last almost forever and is eco-friendly such as solar radiation, geothermal, sea tidal, and wind. Solar energy is radiant energy emitted by the sun which is widely known and used because of its sustainability and applications. Therefore, there are two sorts of solar energy. One is passive (Figure 1.1) and the other is active (Figure 1.2). Passive type is the energy used without utilizing mechanical devices which is applied to indoor applications like making a house faces the sun directly. Active solar energy operates with mechanical units like collector and heat storage for electricity generation, heating and cooling applications, and solar vehicles. The most noticeable projects of this type are photovoltaic panels, concentrating solar power plants for power production, solar thermal energy for heating like gaining hot water for human usage and for cooling like absorption refrigeration cycles where solar radiation is used to heat the chemical components. Among all Active solar energy projects, *SCPP* (solar chimney power plant) or *SUT* (solar upwind tower) comes into the picture like concentrating solar power plants depending on the natural convection concept to gain electricity without utilizing complex parts or devices. It uses the sunray to heat atmospheric air under a collector by natural convection to accelerate the air particles then the air pass through a wind turbine to generate power.

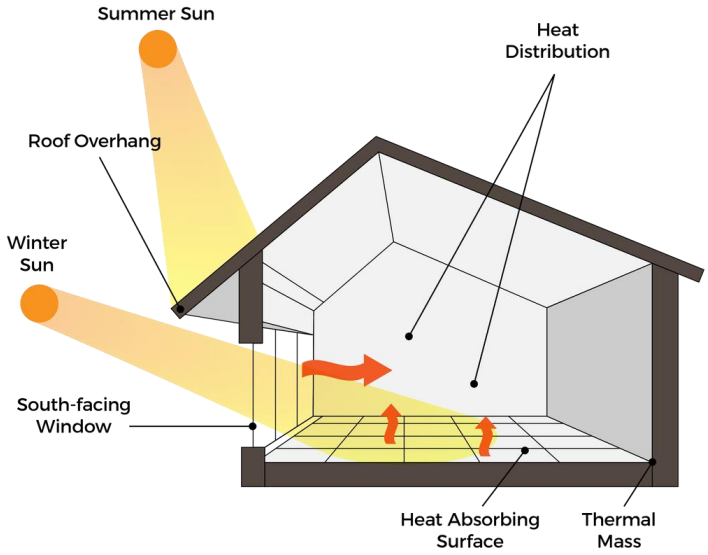

Figure 1.1. Passive solar energy.

Figure 1.2. Active solar energy.

1.1. FREE CONVECTION

Thermal energy is transferred by conduction, convection, and radiation which is occurred from a hot medium to a cold one. Conduction is the energy transfer from high energetic particles to adjacent low energetic particles of a substance where the substance could be gas, liquid, or solid. In gases and liquids, it's appeared as collisions and diffusion of the molecules during their random motion. In solids, it is due to the combination of vibrations of the molecules in a lattice and the energy transport by free

electrons like a hot side and a cold side of a rod. Unlike convection which is the mode of energy transfer between a solid surface and the adjacent liquid or gas that is in motion, it involves the combined effects of conduction and fluid motion where the faster the fluid motion becomes, the greater the convection heat transfer becomes, too. Generally, there are two types of convection heat transfer. It is called forced convection if the fluid is forced to flow over the surface by external means such as a fan, pump, or the wind. In contrast, convection is called natural (or free) convection if the fluid motion is caused by buoyancy forces that are induced by density differences due to the variation of temperature in the fluid. On the other hand, Radiation is the energy emitted by matter in the form of electromagnetic waves (or photons) as a result of the changes in the electronic configurations of the atoms or molecules that is unlike conduction and convection, the transfer of heat by radiation does not require the presence of an intervening medium such as solar radiation [1]. Free convection is well known for its applications where the heat transfers without any velocity interfering in the process like household radiators meanwhile forced convection is based on the use of fluid velocity. Figure 1.3, which is taken from the heat transfer book [1], presents free convection in a vertical hot plate where the fluid starts moving in the boundary layer region to form a curved velocity profile in the zone with almost a linear temperature profile from the plate to the stationary fluid region.

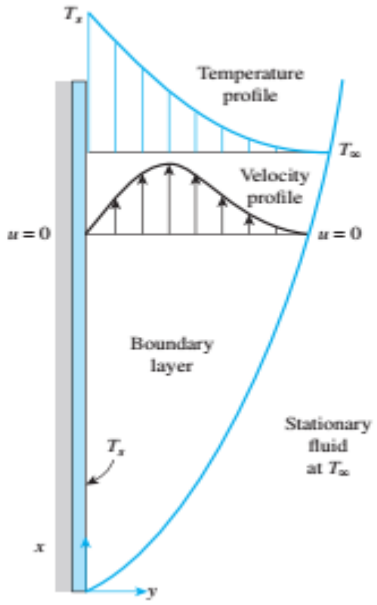

Figure 1.3. Vertical hot plate [1].

To describe the flow motion There are governing equations which are continuity, momentum, and energy, next to other terms which are:

Boussinesq approximation:

It's the density difference between the inside and the outside of the boundary layer that gives rise to buoyancy force and sustains flow [1], in other words, it's the slight change in fluid properties depending on the density variation with temperature.

Grashof number:

Presents the ratio of buoyant forces to viscous forces and includes the Reynolds number, that predicts the flow action whether it is turbulent or laminar, with temperature difference.

Rayleigh number:

Is the product of the Grashof number with the Prandtl number. Here Rayleigh number plays the same role as the Reynolds number for free convection namely it can predict whether the flow is turbulent or laminar.

Nusselt number:

Presents the ratio of heat transferred by convection to heat transferred by conduction. It helps to determine the suitable heat transfer coefficient to maintain the desired rate of heat according to Newton's law of cooling.

Newton's law of cooling:

Expresses the way of heat transfer by convection.

$$\dot{Q}_{conv} = hA_s(T_s - T_\infty) \tag{1.1}$$

As it's noticed heat transfer rate is affected by heat transfer coefficient, A_s Surface area, and temperature difference between mediums.

All previous relations and terms are mentioned in the methodology part later.

1.2. SOLAR CHIMNEY POWER PLANT (*SCPP*)

It's a power plant that counts on the solar radiation to produce air motion (wind) within it by using natural convection to produce power where the air is heated under a collector then moved forward to a wind turbine, and later it's passed through a chimney to get out from the entire system. The plant concept started with a simple idea in a magazine and developed to have the first pilot in Manzanares Spain in 1983 (Figure 1.2) where the pilot gave a very clear idea and results that build the future view of this technology [2,3]. Some of these profits are a long-life span, simple construction, works at all times with no additional components, cheap construction materials, low maintenance price and no require for a solar tracking system nor cleaning system [4], therefore, *SCPP* is in the scope of governments and studies. *SUT* (solar upwind tower) has very simple components where playing with any of them will have a huge impact on the plant output. It can run almost under any weather condition and of course maximizes on sunny days even with wind absence in the area because of the base work principle that the project has. Later on, some other experimental studies come out into field like the one in Canada. These days to minimize the cost of making too many virtual investigations a numerical method was invented in other words computational fluid dynamics as a shortcut is called *CFD* which eases the way of researches and makes them simple.

Figure 1.4. Manzanares pilot [5].

1.2.1. *SCPP* Components

SUT is built from a collector (canopy or glass), tower, absorber (normal ground or any storage type), and wind turbine installed at the base of the tower. Each part has its effect on the plant. The collector is the part responsible for gaining heat and generating buoyant forces that are influenced by its material, shape, elevation, and inclination. The importance of this section comes from the idea of having a huger collector (huger collecting space) leads to more heated air later more power, likewise, the absorber acts as the second assistant to heat the fluid. It's the best place to locate other systems or a rejected heat from other constructions to form a hybrid system like *PV* panels, and different materials sort. The chimney is the exhaust part to reinject the use air to the atmosphere again where its diameter, height and form have a direct impact on power out for example having a longer chimney means higher output. Finally, the turbine is the power production unit which is usually a wind turbine. It could be manipulated easily by changing blade shape like having a symmetric one, number of blades, gears ratio, turbine type, and nubmer of turbines. All of them have a direct or indirect influence on the plant in one way or another with the ability to add more components. After all, *SCPP* is one of the most flexible plants. Figure 1.5 shows the components of *SCPP*.

Figure 1.5. SCPP pilot components [6].

1.2.2. Working Principle of *SCPP*

Natural convection or in other words buoyancy-driven force is one of the most common shapes of heat convection. In this study, buoyancy-driven force is generated under the collector surface because of solar radiation where the air density decreases (becomes lighter). Therefore, the air particles start to move (the velocity is generated) from nowhere. All of that is accompanied with a decrease in pressure because the system is totally an open system and an open cycle then the air moves toward the chimney passing through a wind turbine to generate electricity (Figure 1.6).

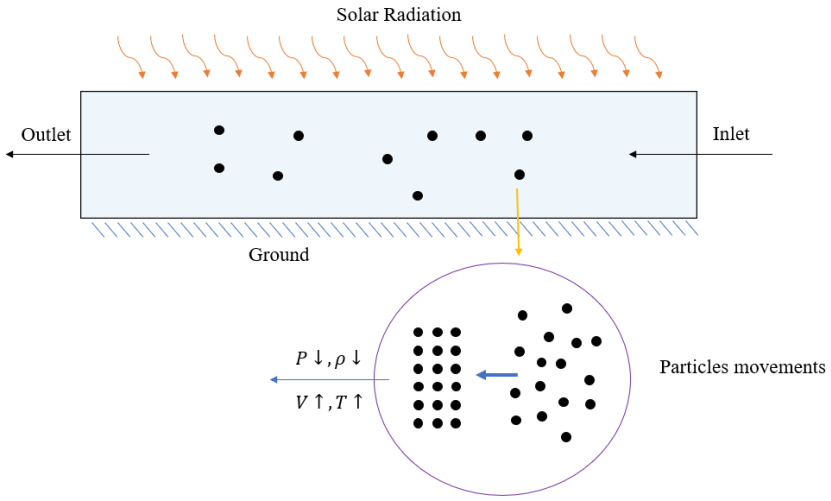

Figure 1.6. Fluid motion.

The entire system represents a huge Brayton cycle. As a result, the collector is like a heater, the turbine is the power generating unit, the chimney is the condenser which is the pressure retrieving part to inject the fluid into the environment at the pressure level and finally, the tower tip to the collector inlet works as a huge compressor [7,8]. Although, all operations are occurring in the troposphere layer, which is 10 km in height, therefore, the air in this situation acts like incompressible fluid leading to getting the tower outlet pressure with simple physical equations and terms. Figure 1.7(a) explains the way how heat is transferred to air and bodies plus how air is affected. On the other hand, Figure 1.7(b) explains the case of the study conducted in this research because the afternoon is the strongest incident sun-ray, i.e., $\dot{Q}_{absorber}$ is negligible which is almost ideal since there is no real total black body.

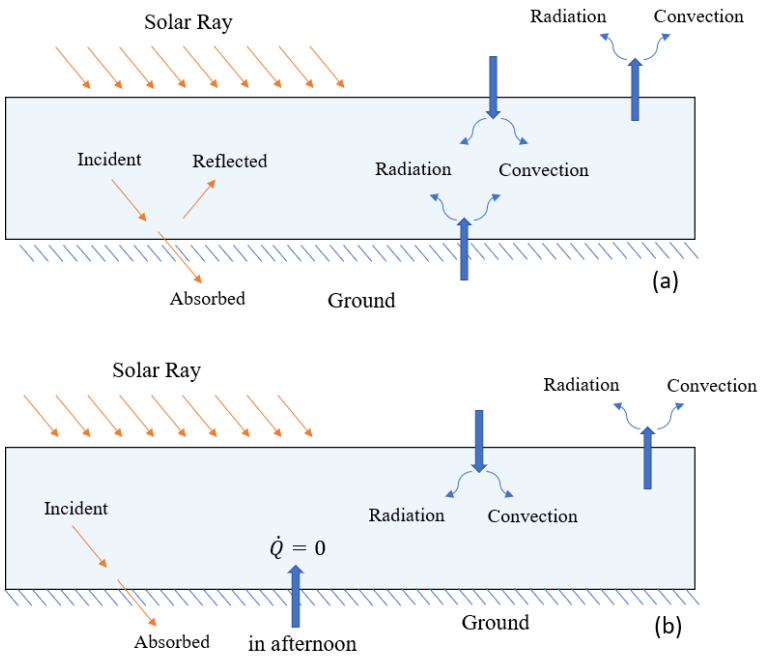

Figure 1.7. Heat transfer methodology [9].

1.2.3. Manzanares Pilot

Schlaich [2,3] in 1983 built the first prototype under the German government control in Spain which is considered as the mother base of the entire works in the following decades. It provided the elements, the shape, and the working principle of *SCPP*, that have been mentioned above, with an unexpected result, which is mentioned in the aim

section. Figure 1.2 and Figure 1.3 show the real concept of the pilot. The research found that to get smooth work there are two conditions should be satisfied. One is the mean temperature distribution of the entire plant should be equal to or higher than 20 ^{o}C. The other is the maximum velocity should be 15 m/s. These conditions shaped the following decades' studies as experimental data.

1.3. LITERATURE REVIEW

For decades *SUT* or in other words, *SCPP* considered an interesting case of study because of its simplicity, advantages, and challenges. As a result, many studies happened and will happen across time to figure out solutions for plant problems or to enhance it.

Some studies tried to implement the idea experimentally. Haaf et al. [2,3] built-in 1983 almost the first real pilot in Manzanares, Spain with its dimensions and the economic feasibility of this experiment under the authority of the minister of research and technology of the German government. Moreover, they found that the system has a very long-life span i.e., it lasts for 7 years more than expected, and other benefits. Furthermore, they put the basic estimations for other researches by keeping in mind $\Delta T \geq 20$ ^{o}C and $V = 15$ *m/s*. In the light of that, they made the solid ground for future investigation later.

Ghalamchi et al. [10] carried out an experimental study on a small-scale model to update the data and to find the best plant dimensions where the model is set to be 3 *m* chimney height and 3 *m* collector diameter. Therefore, it is found that 6 *cm* is the ideal collector entrance elevation, and 3 *m* and 10 *cm* are the ideal chimney tallness and tower diameter, respectively.

Mehdipour et al. [11] discussed in 2020 the opinion of increasing collector diameter virtually by an indoor sample to reduce the influence of continuous climate change. The sample count on the idea of changing the collector angle. Consequently, it’s found that ascending collector radius is not always a good idea.

A very simple concept can change the system like Eryener et al. [12] who experimented a mix of transpired metal and glaze collector to get a 76% collector efficiency which is three times higher than *SCPP* collector efficiency. So, the study aimed to change collector features in order to descent tower height.

Mehdipour et al. [13] conducted two different indoor setups which are a circular collector with a chimney located in the middle and a square collector with a chimney placed at the side of the setup to control environmental conditions easily. It's shown that a square collector has better performance, velocity, Nusselt number, and heat transfer coefficient than the circular one having several problems like secondary flow generation, velocity, hydraulic losses, etc.

Some studies combined the experimental method with the *CFD* technique like Khidhir et al. [14]. It is designed and built a *SUT* integrated with solar reflectors under the collector to improve fluid flow temperature, therefore the reflectors increased maximum air temperature at the chimney base by 10.25% more than usual which led to an increment in fluid velocity by 22.22% and a reduction at its density. Hence the plant power output excessed the usual average outcome by 56.867% at peak time.

Avcı et al. [15] In 2019 an experiment occurred for an inclined collector facility and was compared with a numerical study to evaluate the numerical results. It's concluded that the *CFD* solution is very well matched to experimental data to improve the facility later and the establishing area of the plant has a great effect on it.

Nasraoui et al. [16] built a small-scale pilot to study the effect of chimney inclination on plant performance which has been modified numerically by varying the inclination angle. It's found that the system performance decreases with increasing tower inclination angle more than 3˚, the optimum angle changes with changing the system scale, and an angle around 1˚ gives the best results.

Belkhode et al. [17] constructed a small-scale pilot by taking plant variables which are chimney height, collector height, and so on to optimize and enhance the plant experimentally, mathematically, and numerically. As a result, the collector

temperature is higher than the environment temperature almost by 10 ˚*C*. Plain glass which is used as a collector material better than Acrylic sheet, Polycarbonate sheet, and Crystalline sheets because of its transmissivity that is almost 80% better than the others. Increasing chimney height increased the efficiency, too.

Ayadi et al. [18] compared a manufactured plant which has been built for this study and *CFD* codes to investigate the influence of varying collector elevation on the output power and it's found that the collector elevation affects the power directly where decreasing the collector elevation will generate more power from the system.

RahimiLarki et al. [19] examined environmental crosswind on a tilted chimney experimentally and numerically. A numerical investigation for solar radiation and tower tilt angle on the new concept. Besides those, dimensionless parameters had been developed to evaluate the idea for the large-scale plant. It's resulted that, a low-speed crosswind decreases the outcome power. The inclination angle between 10˚ to 20˚ gives greater performance than the conventional chimney, and for the large-scale, the inclination angle around 15˚ gives higher performance by 5% - 20% depending on the ambient crosswind velocity.

Mokrani et al.[20] manufactured a *SUT* and integrated geothermal water as a secondary heat source located under the collector and above the absorber to test three different cases which are sun ray only in the daytime, geothermal energy only at night time, and the combination of both in the daytime. As result, the solar irradiance case increments collector's temperature to reach 68.3 ^{o}C and the air velocity to be 5.8 *m/s*. Geothermal case rises the temperature to 37.1 ^{o}C and the velocity to 5.1 *m/s*. For the last case, the combination results in an increase in temperature to be 80 ^{o}C and the velocity to be 7.1 *m/s*.

Huang et al. [21] hybridized *SCPP* with *PV* panels in a small-scale pilot and had done the same for a numerical large-scale base on *SCPP*s data by adding suction fans, that are linked to the panels, where panels are placed in two different places. One is above the collector. Another is beneath the collector. It was found that the air flow rate reduces by about 14% with a remarkable boost in outlet power for the experiment. On

the other hand, the simulation way showed an increase in fluid flow rate for the first case of the large scale by 2.21 times more than the traditional *SCPP* and 2.42 times for the second case.

As it can be seen the experiments are always promising and confusing at the same time. For that, a new model should be settled to update the data like *SCPP* one with having the new thoughts within it. Due to the expanses of establishing a new prototype, *CFD* studies appeared in the field.

Some studies investigate parameters enhancement examples for that, Sangi et al. [22] compared between two models, mathematical and numerical using *CFD*, and experimental data of *SCPP* prototype. This study counts on Navier–Stokes, continuity, and energy equation to describe the mathematical model. On the other hand, illustrates standard *k*-epsilon as the turbulent template for *CFD* simulation. Which results that all types approximately have the same results showed by increasing in temperature and velocity with the flow direction and vice versa for pressure.

Yapıcı et al. [9] conducted a *3D* modeling and simulation of *SCPP*, and an intensive study of different parameters effects on *SCPP* which are chimney height, geometry (shape) and diameter plus collector radius, elevation, and inclination angle. The study discusses the best way to get the best performance and the best optimization which leads to that chimney diameter is the most effective factor on the system thus it should have an optimum value to ensure the best performance while increasing the chimney height beside changing in the shape especially diverged form increase the power output and power plant efficiency. Looking at the other side, the collector has a huge impact on the device. Increasing the collector radius will have the same influence as chimney height although raising the collector elevation isn't the best choice because it is considered as the second optimum value of the suit. Collector inclination angle has a conflicted effect, so it's found that 0 angle is the best option.

Babin et al. [23] studied the effect of backflow on the entire setup and it’s found that the air direction is related to pressure and temperature gradients and a farther study should be made to find a solution for back flow situation inside the facility.

Cuce et al.[5] mentioned a better method to simulate *SUT* by using Ansys Fluent to obtain more realistic results and compare them to the Manzanares prototype in Spain. It uses *RNG* $k-\varepsilon$ instead of Standard $k-\varepsilon$ to describe the turbulence inside the system and it develops several correlations to link solar intensity with the main thermo-physical parameter. As a result, the simulation has close results to *SCPP* results. *SCPP* power increases linearly with solar intensity and decreases with the ambient temperature.

Abdelmohimen et al. [24] proposed *SUT* in KSA's weather which is well known as deserts and very dry spaces in different locations numerically. It's concluded that *SUT* runs very well in Bisha region which has the best solar intensity and ambient temperature that meet the *SUT* requirements.

Some focused on the tower. Cuce et al. [25] lighted on the importance of chimney tallness and its effect on overall efficiency which is linear relation whenever the chimney gets taller that means higher efficiency and vice versa and decreasing collector temperature.

Keshari et al. [26] discussed a new technology to improve divergent chimney to optimize the system. *ATSCPP* 'annular tower solar chimney power plant' is a divergent chimney with having several walls inside it like many pipes inside each other with different diameters to reduce and eliminate the boundary layer separation phenomena *'BLS'* causing in pressure and eddies near to tower outlet when the tower exceeds the optimum value. Moreover. It developed that concept due to the high cost of construction. The result shows that the *ATSCPP* has better performance, power output, and efficiency compared with divergent chimney and the developed concept has fewer values than *ATSCPP* by almost 6% and better values than the old type.

Das et al. [27] provided a numerical simulation for different parameters, chimney slope angle, solar radiation, surrounding temperature, and turbine efficiency, and their effects on *SUT* performance with integrating exergy concept into the analysis. In addition to a full comparison between parameters. It's concluded that 2° is the optimum

angle value to get the best results for the system which enhances the power output, net exergy, and overall efficiency.

Others studied the collector. Keshari et al. [28] studied the collector inclination effect on generated power and total efficiency with different models. So, it’s found that the optimum angle is 6˚ and the most suitable turbine place is at 2.5 m height from the chimney base.

Kebabsa et al. [29] proposed a novel solar collector for *SCPP* named as *SCESCPP* (sloped collector entrance *SCPP*). The collector isn't fully sloped but only the entrance by varying sloping angle according to horizontal collector radius to total collector radius and same for collector height. It's found that the system has a better power outcome and better performance.

While some studies conducted both interests (tower and collector). Hassan et al. [30] depicted the effect of having a divergent chimney and sloped collector by using *RNG* $k-\varepsilon$ to get more accurate results and compare it with the *SCPP* plant. It's concluded that there is an optimum value for divergent chimney '1-2°' and 6° for collector part which led to better performance, less height in chimney partition, and smaller collector diameter. Namely, a smaller arrangement with better performance than the conventional suit.

Meanwhile some studies mentioned the turbine influence on the arrangement. Kasaeian et al. [31] varied turbine blades number and angular velocity besides chimney tallness with collector diameter accordingly the increase in angular velocity with blades number will enhance the output in the same hand rising chimney elevation and collector diameter will boost up the power, too.

Zuo et al. [32] studied and figured out the same result as the previous one but with adding economical study which gives the upper hand to a supercharged system over the conventional one.

And so on, there are so many solutions had been introduced and others suggested hybrid systems like Pratap Singh et al. [33]. It is investigated a hybrid system combined from the solar chimney power plant (*SCPP*) and *PV* panels located under the collector instead of the storage layer. The study mentioned four different shapes of *SCPP* hence it's found that the best agreement containing divergent chimney plus an inclined collector gives the highest performance for the entire suit where it provides a high velocity to cool down *PV* panels growing its efficiency and a high outlet power from the installed wind turbine in the system.

Kashiwa et al. [34] estimated a novel method to get freshwater from the environment by using a cyclone method that implemented at the chimney called by solar cyclone. It’s found that one solar cyclone at 500 *m* high can provide household freshwater needs, and 75% of power demand for 10000 humans in dry zones.

Zuo et al. [35] assumed a hybrid system contained a supercharger turbine in the chimney tip with a wind turbine inside the tower, waste heat gas from the ground, and seawater to desalinate besides that a parametric study was carried out to get optimum parameters 200 *rpm*, 6 *m*, 9 *m*, and 60 *m* are turbine angular speed, nozzle tallness, tower outlet radii and tallness of tower mixing part, respectively. Accordingly, 377.9 *kW* and 20.3 *ton/h* are found work outcome and hourly freshwater, respectively. Abdelsalam et al. [36] conducted *SCPP* with desalination seawater by using the working principle of cooling tower installed in the chimney. As a consequence, the new system can produce power around 50% and freshwater 1.5 times higher than traditional *SCPP* moreover it’s more efficient by 1.4 times than the normal suit.

Some research mentioned the *SUT* integrated with energy storage. For instance, Sedighi et al. [37] conducted *SUT* with storage layer to check the effects of solar ray, turbine pressure drop and soil porosity. It’s concluded that an increment in solar intensity drops arrangement pressure and speed up the air velocity, otherwise, the velocity drops with an improvement in turbine pressure ratio. The heat loss decreases with decreasing turbine pressure ratio. To get the best efficiency and power outcome the porosity of soil should be low.

Attig-Bahar et al. [38] studied a *3D SCPP* model in the southern regions in Tunisia and developed a *2D* transient model with *1D* buoyancy driven flow to study the effect of thermal storage more realistically. As a consequence, 35% increase in power production when having a storage. A long-term storage should be designed when designing *SCPP*.

Amudam et al. [39] conducted *3D*-model with different periods and it's found that the solar storage extends the operation and decreases the outcome compared with traditional because the heat is stored during daytime.

Rashidi and Omara [40,41] assessed the usage of phase change materials (*PCMs*) in *SCPP* as thermal storage, and it's concluded that *PMCs* have a respectable impact on plant's efficiency where having a *PMC* with a large phase change temperature difference is more preferable because it can melt earlier than short phase change temperature difference and using *PMCs* with small melting temperature are more favorable because they can charge and discharge in easily. paraffinic *PCMs* are recommended for utilization in urban regions.

Méndez et al. [42] simulated the system with *COMSOL* Multiphysics to compare between *PMC*, phase change materials, and solid materials as system storage to boost the arrangement. It's concluded that bismuth-led-tin-cadmium and magnesium chloride hexahydrate are the best between all *PMCs* likewise sandstone is the best through whole solid materials.

To get a farther level of advancement Ashouri et al. [43] combined *PMC* with fined absorber surfaces and *PV* panels to test the impact of changing the previous technologies on *SUT* outcomes in residential areas. It's found that an increment in *PMC* mass enlarges ventilation capacity, period and power production fined surface and vice versa for un-fined absorber. This system with Sodium Acetate Trihydrate/Copper Foam as *PMC* can generate power more than *SCPP* with *PV* panels only by 19.8%. it's discovered that Sodium Acetate Trihydrate/Copper Foam (*SAT/CF*) and paraffin/copper (*Pa/CF*) are the best for commercial unitization in urban zones.

Hosseini et al. [44] studied the effect of absorber rectangular fins and varying their dimensions and design on the entire facility. As a result, too many fins and high fins increase heat transfer and efficiency. Unlike, fin thickness where an increase in it decreases the outputs.

Cottam et al. [8] analyzed the system by using thermodynamics, *MATLAB* numerical model, and simple cost study to get the best configurations for the suit where the collector and chimney radiuses have the main impact on pressure drop ratio otherwise the chimney height influences the power output directly all of that under good match compartments namely with their dimensions for that assorted plants with 3000 *m* better than a large scale once.

It can be seen from literature review that there are a lot of studies with different solutions to improve the *SCPP*. With taking the collector changing method into account this work tries to add fins to the rooftop and varies it to enhance the total system which is considered as a new method of development, i.e. A new collector type that shares the same idea with [44] but in a different location accounting on [5,9,27] to have the *CFD* steps and methodology besides that the results were validated with [27,45,46].

1.4. OBJECTIVE AND AIM OF THE STUDY

SCPP's benefits are facility simplicity, harvesting energy in arid areas or deserts, the ability to work at night without having additional components or materials (heat transfer fluid or molten salts), the ability to grow plants in dry areas (agriculture), numerous development choices, long life span, very low maintenance expenses with almost anyone can make the power plant and cheap materials with cheap constructing cost. All of that made this study within the scope of many governments to get sustainable and clean energy. On the other hand, this study is still facing some challenges such as the chimney elevation, collector surface area, total space that the project uses, how the facility can resist wind on windy days, especially with a long tower or desert storms, and low thermal efficiency. Because of those advantages and

disadvantages, the plant could be optimized and enhanced so easily which opens the door to farther research and investments with uncountable ways to develop.

The major works try to investigate the impact of changing plant parameters and others to add some other parts to get higher efficiency and power output which is the main aim of all of the research. But a few of them tries to minimize the facility size with having better outcomes, efficiency and power, in the light of that fact there are two efficient ways to improve the system. One is customizing the collector with new technologies or applying a traditional simple, efficient and experimented ways. Another is by adjusting chimney or inventing new methods especially tower height is a series issue limiting the plant abilities i.e. The chimney could be higher than Eiffel tower. If the chimney would be less in tallness. The collector size will be bigger to obtain a better work outturn. From the collector's perspective adjusting it with a constant chimney height will get the same goal as the tower one. The reason behind choosing these two methods is the direct impact on the desirable goals where a larger collector means more heat gain and a higher tower means a higher outcome.

The tower could be minimized so easily and cheaply with different technologies [26] and the collector could be resized by using fins installed in it which is a novel rooftop. It is indicated in this study to get more heat or the same amount of heat with a smaller rooftop size. Besides that, a parametric study is carried out to get the optimum dimensions of fins and the best solution.

PART 2

METHODOLOGY

Many studies conducted the arrangement for years. According to [2,3] various models were investigated by different methods. One of them is a *3D* model carried out by [5,9,27,28,47]. This section discusses the working steps of the same way to simulate the plant and how to enhance its natural convection and thermal efficiency. Firstly, the *SCPP* pilot is simulated then validated by comparing the results with experimental data. Later on, the new concept (fined collector surface) has been applied.

2.1. PROBLEM DESCRIPTION

This part discusses the plant, the computational domain and dimensions. Figure 2.1 shows schematic view of *SCPP* pilot. Dimensions of *SCPP* pilot is also given in Table 2.1. According to the aim of this study *SCPP* could be modified so easily which affects the plant performance directly. The huge issue of this plant is related to the low amount of heat gained and the huge amount of heat loss from the collector part so fins were installed in the collector to enhance the amount of heat gained and decrease the losses which leads to have small collector with a better heat gained amount.

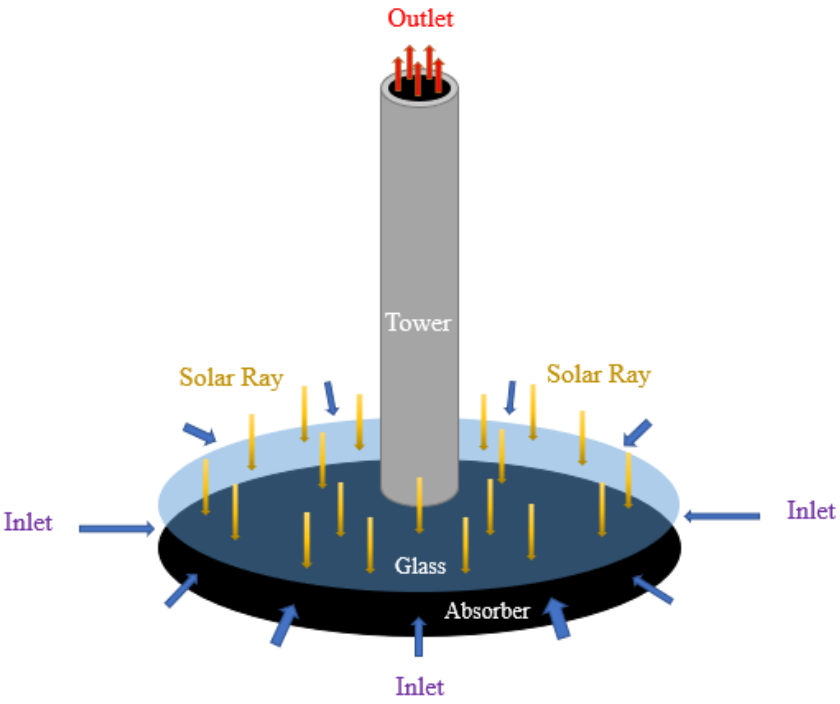

Figure 2.1. *SCPP* schematic [2].

2.1.1. *SCPP* Pilot

Figure 2.2, Figure 2.3, and Table 2.1 describe the pilot dimensions and shape. Since using Ansys 2020R2 beside the circular form of the structure a quarter shape was used after drawing the full model (Figure 2.4). The quarter body was obtained by a *2D* sketch was drawn on the *XY* plane and revolved by revolve command about the *Y*-axis, then the symmetry tool was implemented twice, one on *XY* plane and the other on *ZY* plane. To get a correct result there is a nick (arc) between the absorber and the chimney axis (*Ch/A)* which is double in size compared to the other one between chimney and collector (*Ch/C)* obtained by filet order, i.e., arc radius of absorber and chimney *(Ch/A)* = 2*arc radius of collector and chimney *(Ch/C).*

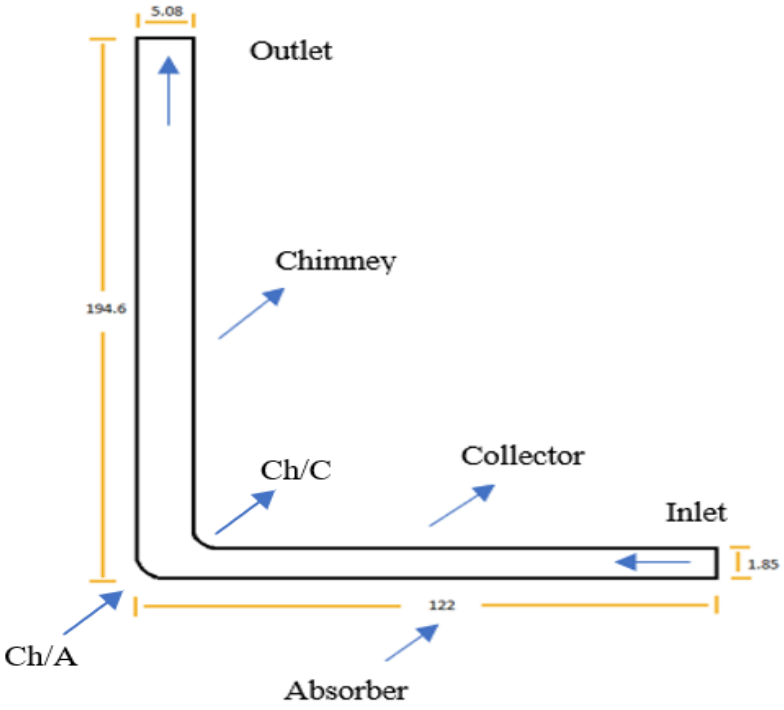

Figure 2.2. Side view of solar chimney power plant [2].

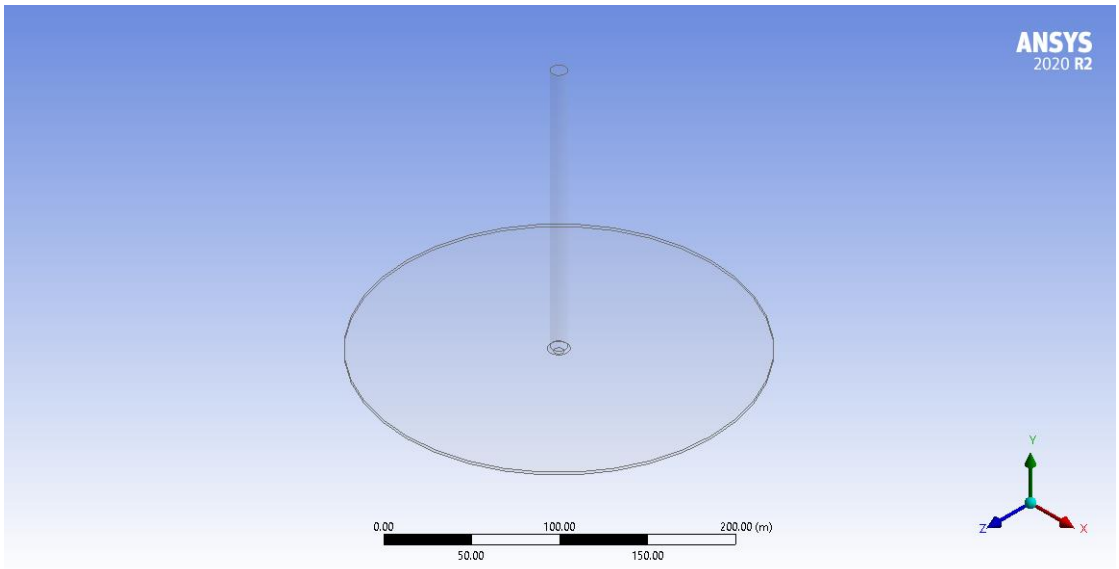

Figure 2.3. *SCPP* geometry [5].

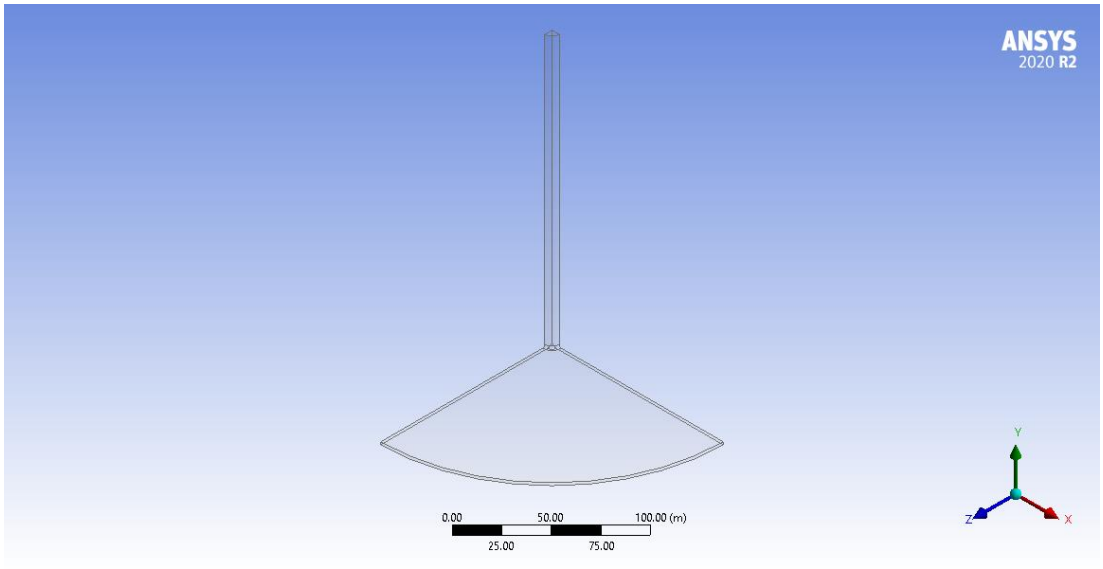

Figure 2.4. Computational domain [5].

Table 2.1. *SCPP* Dimensions [2].

Tower height	194.6 *m*
Collector height	1.85 *m*
Collector radius	122 *m*
Chimney radius	5.08 *m*
Ch/C filet	1.5
Ch/A filet	3

2.1.2. Fined Surface

Figure 2.5 and Figure 2.6 show fin dimensions and application. Figure 2.7. and Figure 2.8 indicate the full and quarter computational domain of fined surface. Table 2.2 and Table 2.3 conduct fin dimensions and variables for parametric study. Firstly, the *SCPP* prototype is built then the fin sketch is added on *ZY* plane. Secondly, extruding the previous sketch to 0.25 *m* which will be changed according to parametric study later. Thirdly, a pattern tool is used to get different fin numbers for the same reason again. Finally, the subtract Boolean is used to combine all bodies in one body.

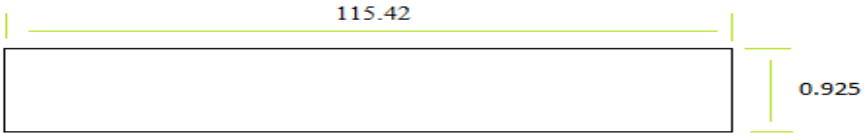

Figure 2.5. Fin dimension.

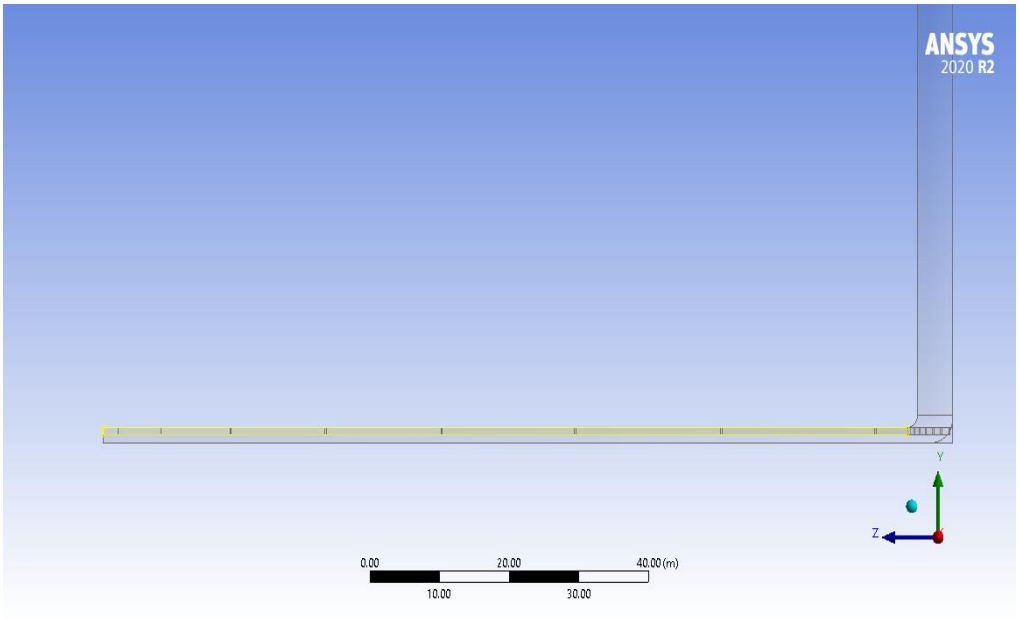

Figure 2.6. Computational domain of finned surface.

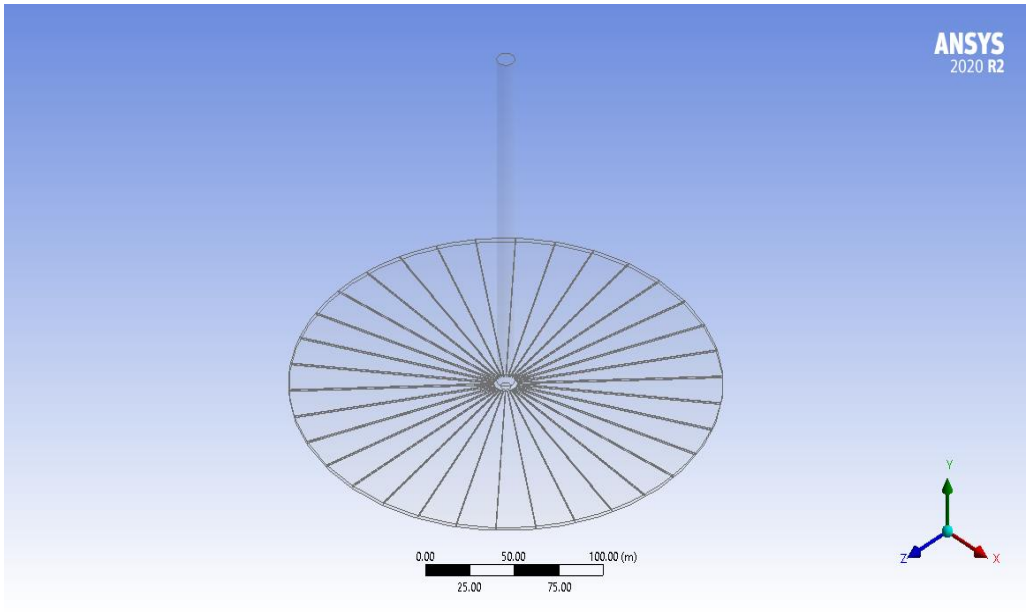

Figure 2.7. 3D view of computational domain of finned surface.

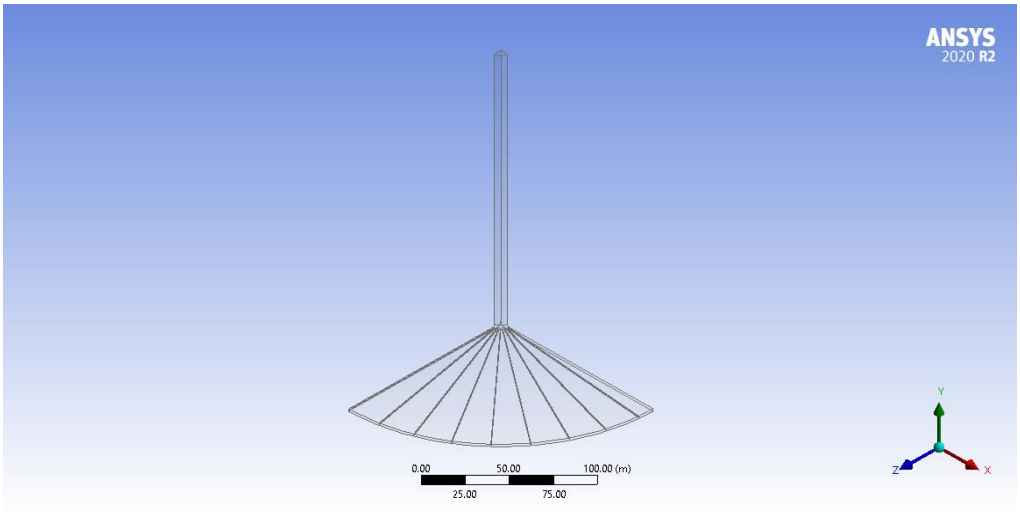

Figure 2.8. Quarter view of computational domain of finned surface.

Table 2.2. Fin dimensions.

Fin height, h	0.925 *m*
Fin width, w	115.42 *m*
Fin thickness, t	0.25 *m*
Number of fins	33

Table 2.3. Fins parametric study variables

Fin height	0.6	0.925	1.2
Fin thickness	0.1	0.25	0.5
Number of fins	25	33	46

2.2. ASSUMPTIONS

- Steady and incompressible
- Inlet and outlet have the same atmospheric pressure condition
- Boussinesq approximation
- Constant solar heat flux I=1000 W/m^2 Time is 1 PM on July the first with location longitude -3.3716˚ and latitude 39.0043˚ with 1 GMT

2.3. MATERIALS

EES (Engineering Equation Solver) is used to get the properties close as possible. Glass is low-iron soda-lime glass. The concert is used as absorption materials where concert properties are taken under T=300 K and P=1atm. Aluminum is used for the tower. The Boussinesq approximation is used for natural convection condition. Some thermophysical properties of the properties used in the study are given in Table 2.4 [1,48].

Table 2.4. Materials properties [1].

Property	Air	Glass	Concert	Aluminum
Density (kg/m^3)	1.169	2530	2300	2699
Specific heat (J/kg.K)	1005	880	880	904
Thermal conductivity (W/m.K)	0.0258	0.937	1.4	235.2
Viscosity (kg/m.s)	1.867e-05	-	-	-
Absorption coefficient	-	58.153	-	1.453e+08
Reactive index	1	1.5129	1	1.0972
Thermal expansion (1/K)	0.003311	-	-	-

2.4. STUDY EQUATIONS AND BOUNDARY CONDITIONS

This part mentions all study formulas and boundary conditions to get Nusselt number and thermal efficiency [1,5].

2.4.1. Governing Equations

These equations present the arbitrary motion of the flow. Each one has been solved by iteration method in *CFD* codes until reaching the converged level to maintain an approximated realistic value.

- Continuity:

$$\nabla(\rho\vec{V}) = 0 \tag{2.1}$$

- Momentum:

$$\nabla(\rho\vec{V}\vec{V}) = -\nabla P + \nabla\left(\mu\left[(\nabla\vec{V} + \nabla\vec{V}^T) - \frac{2}{3}\nabla\vec{V}I\right]\right) - \rho\beta(T - T_0)\vec{g} \tag{2.2}$$

- Energy:

$$\nabla\left(\vec{V}(\rho E + P)\right) = \nabla\left(\lambda_{eff}\nabla T - h\vec{J} + \left(\mu\left[(\nabla\vec{V} + \nabla\vec{V}^T) - \frac{2}{3}\nabla\vec{V}I\right]\vec{V}\right)\right) \tag{2.3}$$

2.4.2. Standard *k*-*ε* Turbulence Equations

The standard *k*-*ε* model describes the turbulent flow of fluid especially fully turbulent flow with omitting the effect of molecular viscosity. It's chosen as solving model to solve governing equations for turbulent flow in *CFD* because of the fully turbulent condition that the plant runs through and its simplicity where the computer doesn't straggle to achieve the desired results.

$$\frac{\partial}{\partial t}(\rho k) + \frac{\partial}{\partial x_i}(\rho k u_i) = \frac{\partial}{\partial x_j}\left(\left(\mu + \frac{\mu_t}{\sigma_k}\right)\frac{\partial k}{\partial x_j}\right) + G_k - G_b - Y_M - \rho\epsilon + S_k \tag{2.4}$$

Rate of the turbulent kinetic energy equation:

$$\frac{\partial}{\partial t}(\rho\varepsilon) + \frac{\partial}{\partial x_j}(\rho\varepsilon u_j) = \frac{\partial}{\partial x_j}\left(\left(\mu + \frac{\mu_t}{\sigma_\epsilon}\right)\frac{\partial\varepsilon}{\partial x_j}\right) + C_{1\epsilon}\frac{\epsilon}{k}(G_k + C_{3\epsilon}G_b) - C_{2\epsilon}\rho\frac{\epsilon^2}{k} + S_\epsilon \tag{2.5}$$

Where:

G_k: generation of turbulence kinetic energy due to the mean velocity gradients.
G_b: generation of turbulence kinetic energy due to buoyancy.

Y_m: the contribution of the fluctuating dilatation in compressible turbulence to the overall dissipation rate.

$C_{1\epsilon}$, $C_{2\epsilon}$ and $C_{3\epsilon}$: constants.

σ_k and σ_ϵ: turbulent Prandtl numbers.

S_k and S_ϵ: user-defined source terms.

2.4.3. Boussinesq Approximation:

It's related to temperature difference and volume expansion coefficient at constant pressure as following:

$$\rho_\infty - \rho = \rho\beta(T - T_\infty)\ at\ P = cost \tag{2.6}$$

$$\beta_{ideal\ gas} = \frac{1}{T} \quad (1/K) \tag{2.7}$$

P [Pa], ρ_∞ [kg/m^3], T [K], T_∞ [K], and β [$1/K$] are density, the density of free stream, temperature, ambient temperature, and volume expansion coefficient, respectively.

2.4.4. Boundary Conditions:

Table 2.5 gives simultion boundary conditions.

Table 2.5. Boundary conditions [5,9,25].

Boundaries	Type	Option	Value
Inlet	Pressure-inlet	-	$P_o = P_{inlet} = 0\ Pa$ as gauge
Outlet	Pressure-outlet	-	$P_o = P_{outlet} = 0$
Absorber	Wall	thermal	$Q = 0\ W$ and $t = 0.5\ m$
	Wall	radiation	Opaque, $\alpha = 0.6$ and $\varepsilon = 0.88$
Chimney	Wall	thermal	$t = 0.0012\ m$
	Wall	radiation	Opaque, $\alpha = 0.09$ and $\varepsilon = 0.03$
Collector	Wall	thermal	Mixed, $h = 5\ W/m^2.K$, $T = 302\ K$, $\varepsilon = 0.854$ and $t = 0.005\ m$
	Wall	radiation	Semi-transparent, $I = 1000\ W/m^2$, Beam direction $y = -1$, $\alpha = 0.20754$ and $\tau = 0.79246$

2.4.5. Grashof Number

$$Gr_l = \frac{g\beta(T_s - T_\infty)L_c^3}{v^2} \quad (2.8)$$

$$L_c = \frac{A_s}{P} \quad (2.9)$$

$$L_c = \frac{D}{4} \text{ For horizontal circular surface} \quad (2.10)$$

$$v = \frac{\mu}{\rho} \quad (2.11)$$

Where;

Gr: Grashof number, v [m^2/s]: kinematic viscosity, μ [N/m^2]: dynamic viscosity, g [m/s^2]: gravity, T_s [K]: surface temperature, T_∞ [K]: free-stream temperature, D [m]: diameter, L_c [m]: characteristic length, A_s [m^2]: surface area.

2.4.6. Rayleigh Number

$$Ra_L = Gr_L Pr \quad (2.12)$$

where; *Ra*: Rayleigh number, *Gr*: Grashof number, *Pr*: Prandtl number.

2.4.7. Nusselt Number

$$Nu = \frac{h\,L_c}{k} = CRa_L^n \quad (2.13)$$

Where;

Nu: Nusselt number, *Ra*: Rayleigh number, h [$W/m^2.K$]: heat transfer coefficient, k [$W/m.K$]: conductivity, C and n: constants.

2.4.8. Turbine Work

The turbine power is expressed as following equation [1,48]:

$$\dot{m}(\bar{h}_1 + \frac{V_1^2}{2} + gz_1) = \dot{m}(\bar{h}_2 + \frac{V_2^2}{2} + gz_2) + \dot{W}_{out} \quad (2.14)$$

where $\dot{m}$ $[kg/s]$ is the mass flow rate, $\bar{h}$ $[J]$ is the static enthalpy, V $[m/s]$ is the velocity, $Z[m]$ is the elevation, and $\dot{W}_{out}$ $[W]$ is the output power, hence:

$$\dot{W}_{out} = \dot{W}_{turbine} \quad (2.15)$$

2.4.9. Heat Rate

The total heat rate is obtained from the sun ray as the following:

$$\dot{Q}_{in} = \pi R^2 I \quad (2.16)$$

Where $\dot{Q}_{in}$ $[W]$ is the total solar heat flux, I $[W/m^2]$ is the solar ray rate, and R $[m]$ is the collector radius.

2.4.10. Efficiency

It indicates how well an energy conversion or transfer process is accomplished.

$$\eta = \frac{Desired\ output}{Required\ input} = \frac{\dot{W}_t}{\dot{Q}_{in}} \quad (2.17)$$

2.5. EXPRESSIONS IN CFD POST

Nu = (areaAve(Surface Heat Transfer Coefficient)@collector*lc)/areaAve(Thermal Conductivity)@collector

Ra = Gr*areaAve(Prandtl Number)@collector

Gr = (g*beta*((areaAve(Temperature)@collector)-(areaAve(Temperature)@medium plane))*(lc^3))/(kv^2)

β =1/areaAve(Temperature)@collector

lc =length()@diameter/2

ν = areaAve(Dynamic Viscosity)@collector /areaAve(Density)@collector

where diameter is collector radius.

η = Wt/Qin

W_t = Ein-Eout

Ein=massFlow()@turbine*(areaAve(StaticEnthalpy)@turbine+((areaAve(Velocity)@turbine ^2)/2)+g*3[m])

Eout=massFlow()@turbine*(areaAve(StaticEnthalpy)@outlet+((areaAve(Velocity)@outlet^2)/2)+g*194.6[m])

Qin = pi*(length()@diameter^2)*1000[W/(m^2)]

2.6. NUMERICAL MODEL

This section conducts steps of simulation according to Ansys 2020R2 for the main plant and the fined collector surface.

2.6.1. Mesh

Figure 2.9 and Figure 2.10 present *SCPP* and fined collector meshes. To obtain the best results free mesh is used. Element order is set to Quadratic and element size is 0.925 which is half of the collector height.

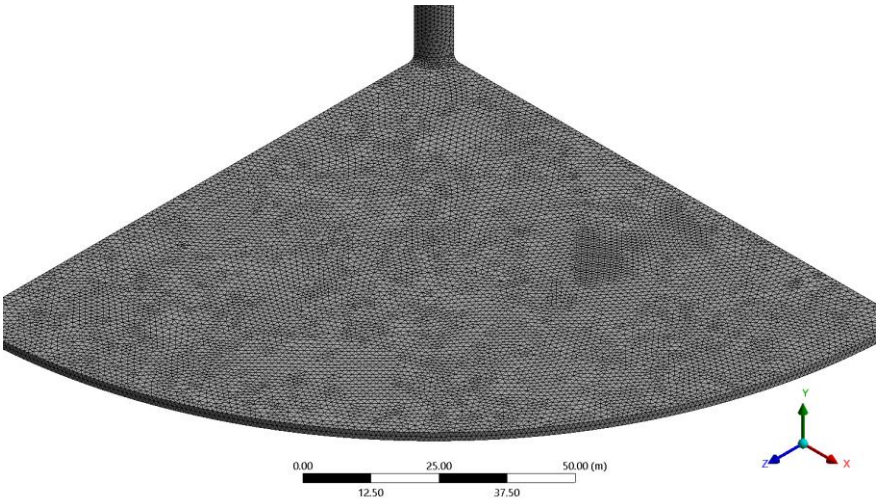

Figure 2.9. *SCPP* collector mesh.

Adaptive sizing is enabled. Quality is set to high and the skewness is 0.79366. The number of elements: 138897.

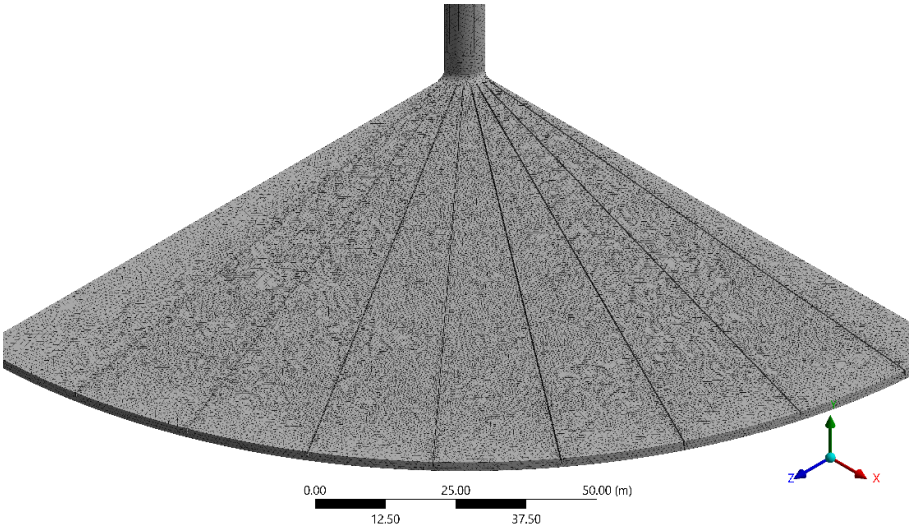

Figure 2.10. fined collector mesh.

The same options are used for the fined collector, but the skewness is increased to reach 0.84204 as max value and the number of elements is increased to be 536619 which performs the smoothest simulation.

2.6.2. Solution

The whole simulations run under the same conditions for *SCPP* pilot [2,3]. $T_{ambient}$ = 302 *K* and P_o = 1 atm are the operating temperature and pressure, respectively.

2.6.3. Models

The enabled models are:

- Energy equation.
- standard *k-ε* model with standard wall function.
- *DO* radiation model with solar calculator.

Solar calculator data:

The longitude -3.3716˚ and latitude 39.0043˚ with 1 GMT Date: 1/7 at 1:00 pm, mesh orientation: East *X*=1, North *Z*=1 (Figure 2.11).

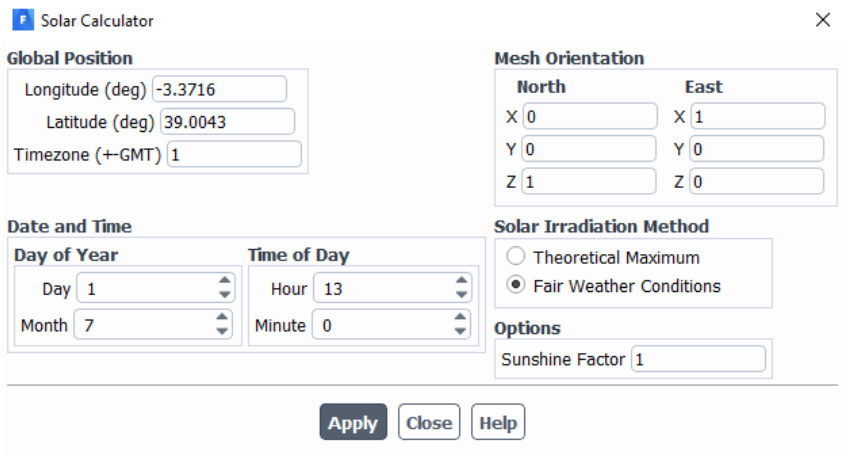

Figure 2.11. Solar calculator.

2.6.4. Reference Values

It should be noticed that the reference is taken from inlet values with V= 0 *m/s*, P = 0 *Pa*, and T=302 *K*.

2.6.5. Methods

- Pressure-velocity coupling: coupled.
- Gradient: green-gauss cell-based.
- Pressure: presto.

All other things are second-order upwind to get more accuracy and the pseudo transient is un-checked.

2.6.6. Solution Controls

The solution control parameters are given in Table 2.6.

Table 2.6. Under relaxation factors.

Flow courant no	200	***Momentum***	0.5
Pressure	0.5	***Density***	0.7
Turbulent dissipation	0.7	***Turbulent viscosity***	0.7
Discrete ordinates	0.7	***Body forces***	0.7
Turbulent kinetic	0.7	***Energy***	0.9

2.6.7. Residuals

All the precisions are set to 0.001 even *DO* except energy is 10^{-6} (Figure 2.12). These residuals are applied for the prototype and the fins. However, for the parametric study, the energy residual has been descendant to 10^{-5} due to the hard convergence for 10^{-6}, it's replaced by 10^{-5}.

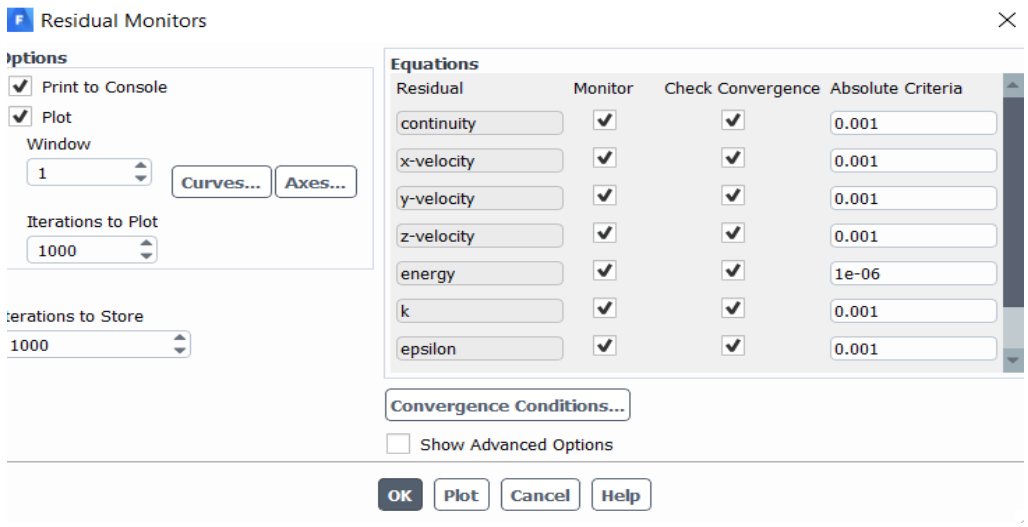

(a)

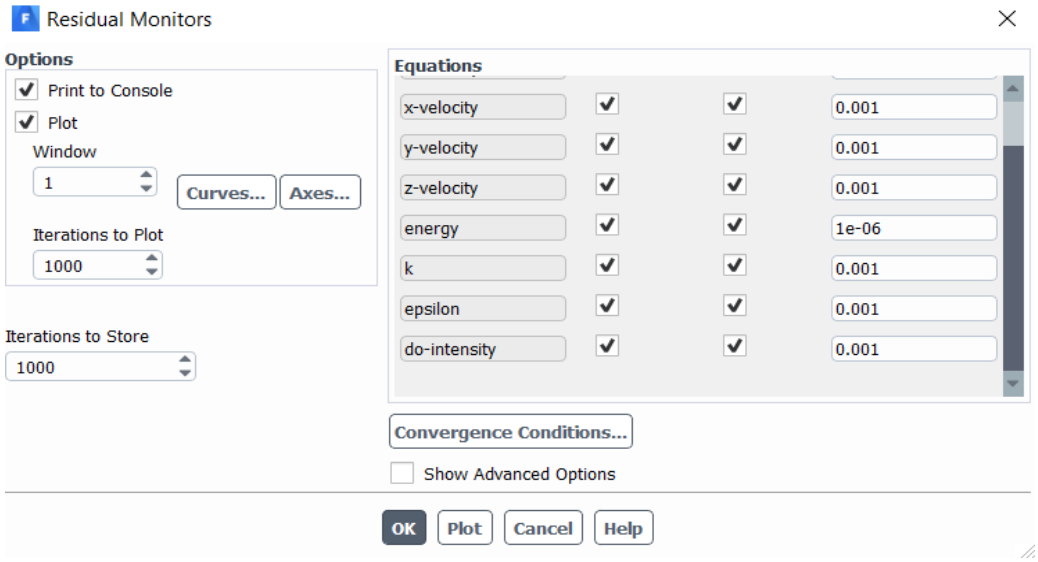

(b)

Figure 2.12. Residuals.

2.6.8. Initialization

The standard initialization is applied from inlet data.

2.6.9. The Number of Iterations

The iterations are set to 10000 times.

2.7. MESH VALIDATION

Mesh Validation is the way to ensure that the solution is correct for advancing the system where a mesh verification should be made by comparing the experimental data results [2] and the simulated one. The comparison counts on the ΔT_{mean} and velocity for the entire suit where ΔT_{mean} is the temperature difference according to the surrounding temperature.

$$\Delta T_{mean} = \frac{SCPP\ maximum\ temperature - \text{ambient}\ temperature}{2} = \frac{T_{max} - T_{ambient}}{2} \qquad (2.18)$$

According to Table 2.7 ΔT_{mean} for *SCPP* is equal to 20 *K* or higher, and the velocity is equal to 15 *m/s*. The simulation gives ΔT_{mean} as 21 and velocity as 15.227 *m/s*. As a result, the mesh is verified. All of that have been occurred with smooth convergence (Figure 2.13).

Table 2.7. Mesh validation.

	Manzanares	**simulation**
$\boldsymbol{\Delta T_{mean}}$	≥ 20	21
V m/s	15	15.227

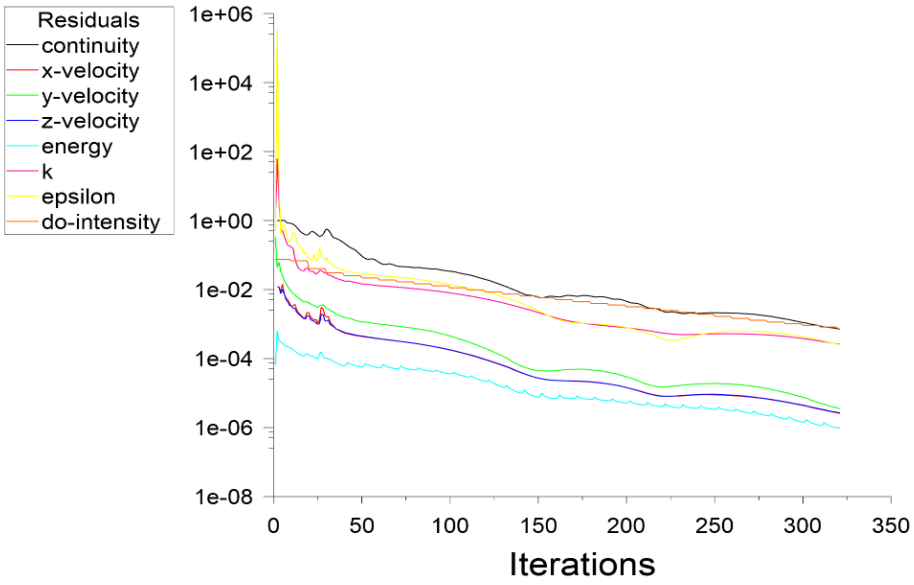

Figure 2.13. Residuals and iterations.

2.8. MESH ADAPTION

Since the mesh is verified to obtain better results a mesh adaption procedure has been happened depending on temperature gradient [5,27]. Figure 2.14 and Table 2.8 discuss the mesh independence. Since the slight differences between meshes then 138897 is selected as the optimum mesh to go on with it. The error percentages which are mentioned in Table 2.8 is studied by the following correlations:

$$\Delta T_{error} = \frac{|\Delta T\ from\ data - \Delta T\ from\ simulation|}{\Delta T\ from\ simulation} \times 100 \tag{2.19}$$

$$V_{error} = \frac{|V\ from\ data - V from\ simulation|}{V\ from\ simulation} \times 100 \tag{2.20}$$

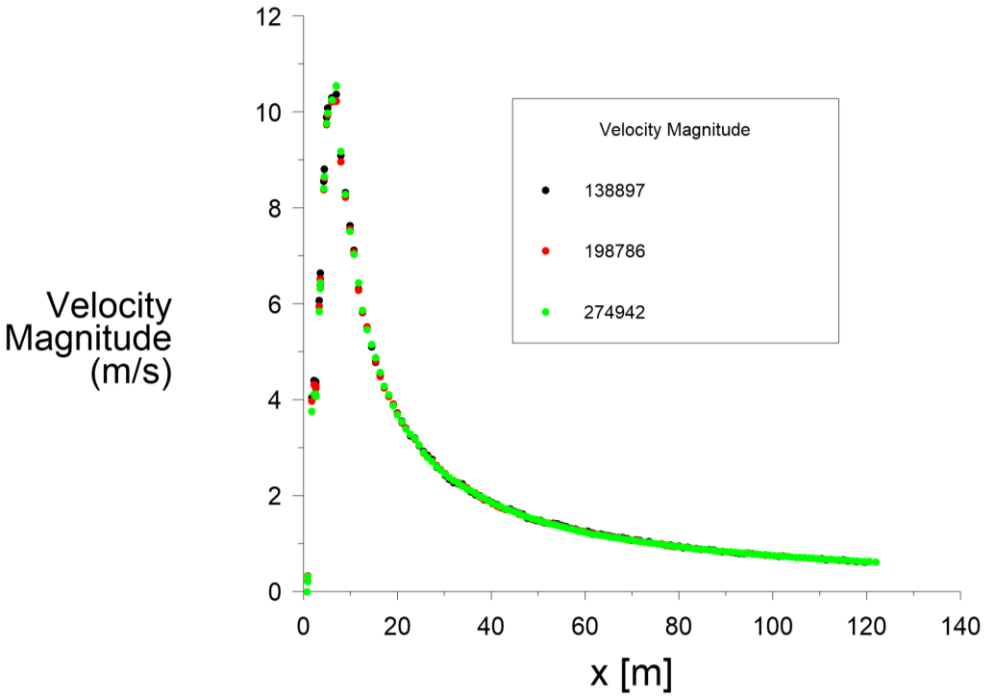

Figure 2.14. Mesh adaption study.

Table 2.8. Mesh adaption study.

Cells number	**ΔT_{mean}**	**Temperature *[K]***	**Velocity *[m/s]***	**Error percentage in V %**
138897	21	344	15.227	1.4907
198786	24.1047	350.2094	15.1623	1.0704
274942	24.1608	350.3216	15.1602	1.0567

PART 3

RESULTS AND DISCUSSION

This section shows the simulation result of *SCPP* and how the adapted solution can affect the system's outputs furthermore a parametric study has been occurred to determine the idea of feasibility with changing fins height, thickness and number.

3.1. *SCPP* PILOT SIMULATION

Three main properties that can control and define the *SCPP*. That are temperature, velocity and pressure. Figure 3.1, Figure 3.2, and Figure 3.3 visualize the air movement where it starts with zero velocity from the inlet and developed slowly to reach the maximum in the tower base. Then losing that velocity slowly again until reaching the chimney tip. All of that occur because of the heating process under the collector, where the air density decreases and the velocity increases. As a result, the best place to locate the turbine is in the tower base (in the tower nick).

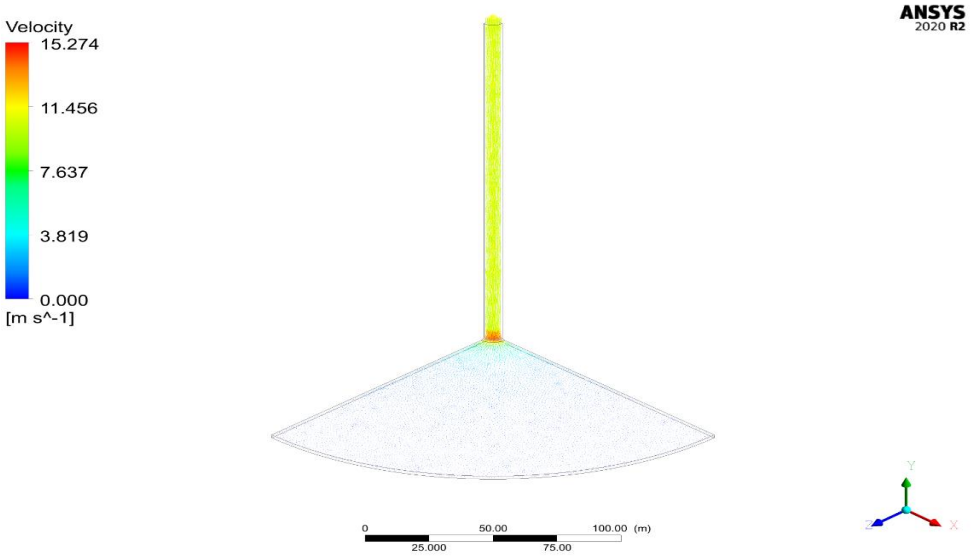

Figure 3.1. Velocity vector of the *SCPP*.

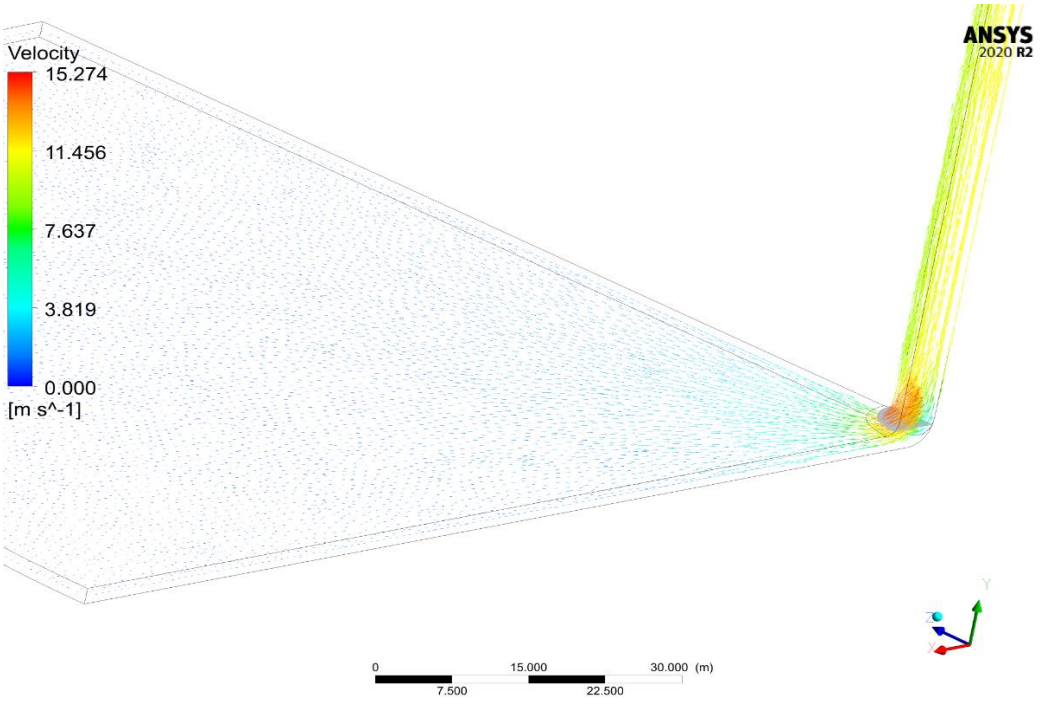

Figure 3.2. Velocity vector side view.

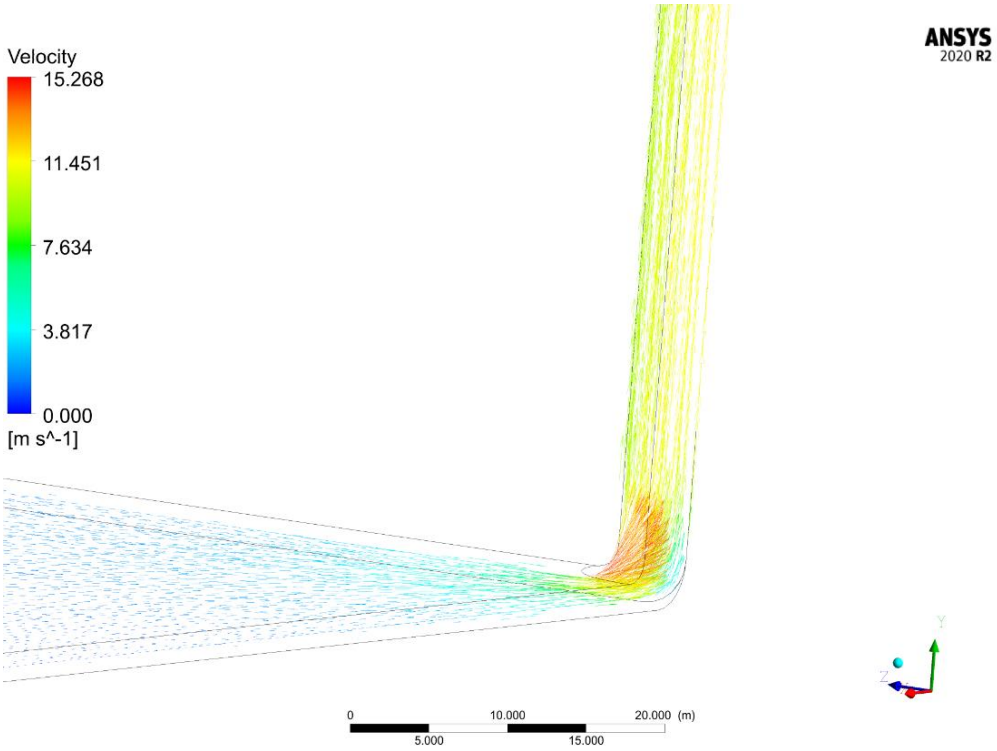

Figure 3.3. Velocity vector tower base.

Figure 3.4 and Figure 3.5 point to the hottest place in *SCPP* and how natural convection happens. Figures show that the air temperature is gradually increases under the sun ray with almost no effect of absorber temperature because of the afternoon condition. This situation highlights the importance of the collector part until reaching the maximum temperature in the outlet of the collector. In this procedure, the air potential energy is converted to thermal and kinetic energies. Later on, the temperature acts like velocity i.e., decreasing gradually to be like the environment.

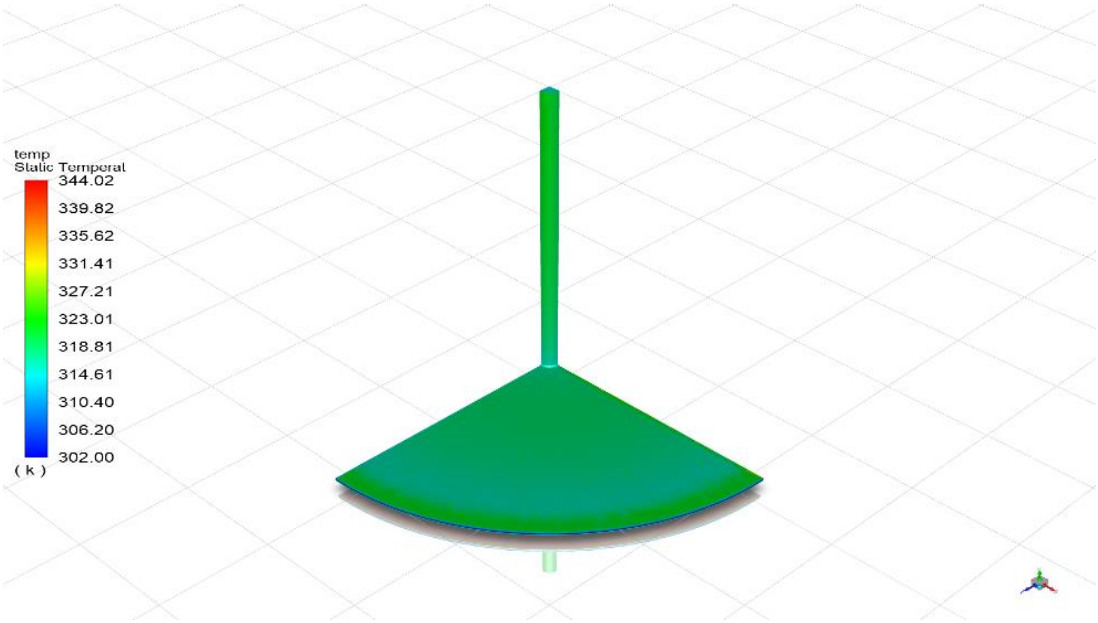

Figure 3.4. Temperature distribution in *SCPP*.

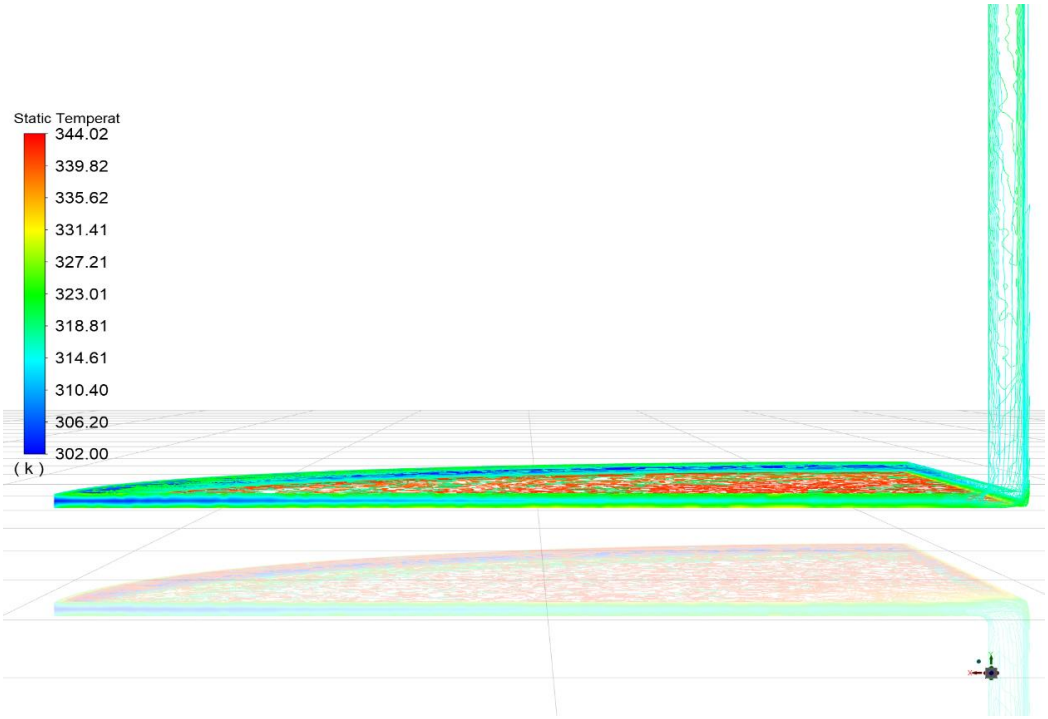

Figure 3.5. Temperature distributions side view.

Figure 3.6 and Figure 3.7 present the pressure distribution in *SCPP*. The air pressure is atmospheric in the plant inlet then decreases gently until approaching the chimney inlet. In the chimney base, the pressure gets the minimum value then increases gently again until reaching the chimney outlet where the pressure is atmospheric again. All of that happens because of the heating process under the collector where decreasing in density comes with an increase in velocity accordingly the pressure decrement. In other words, the system runs under a vacuum pressure. But at the same time, it can't be called a vacuumed system because of the tropospheric layer of earth (the air acts like incompressible flow).

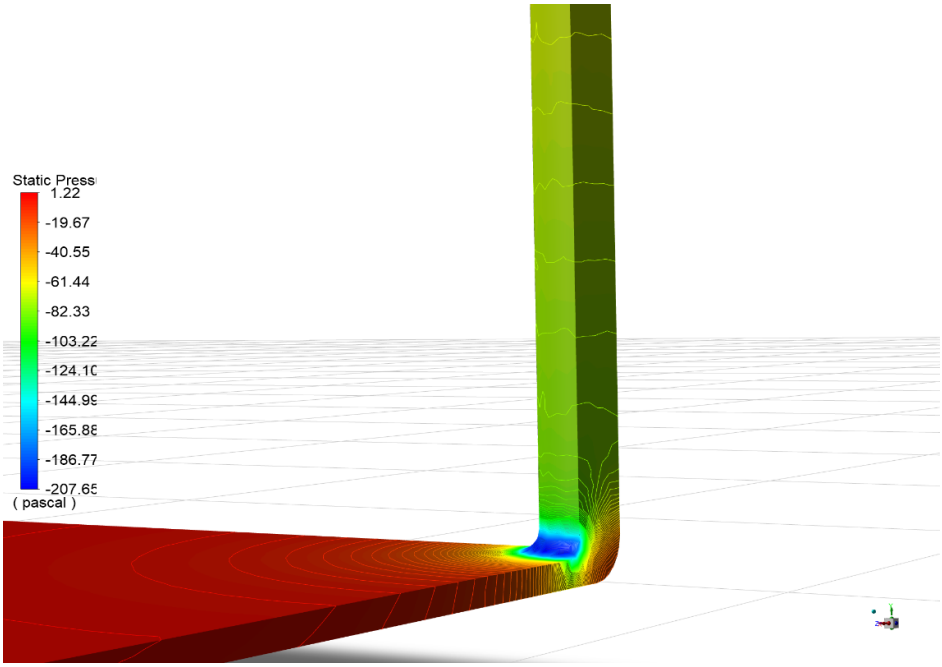

Figure 3.6. Pressure distribution on the tower base.

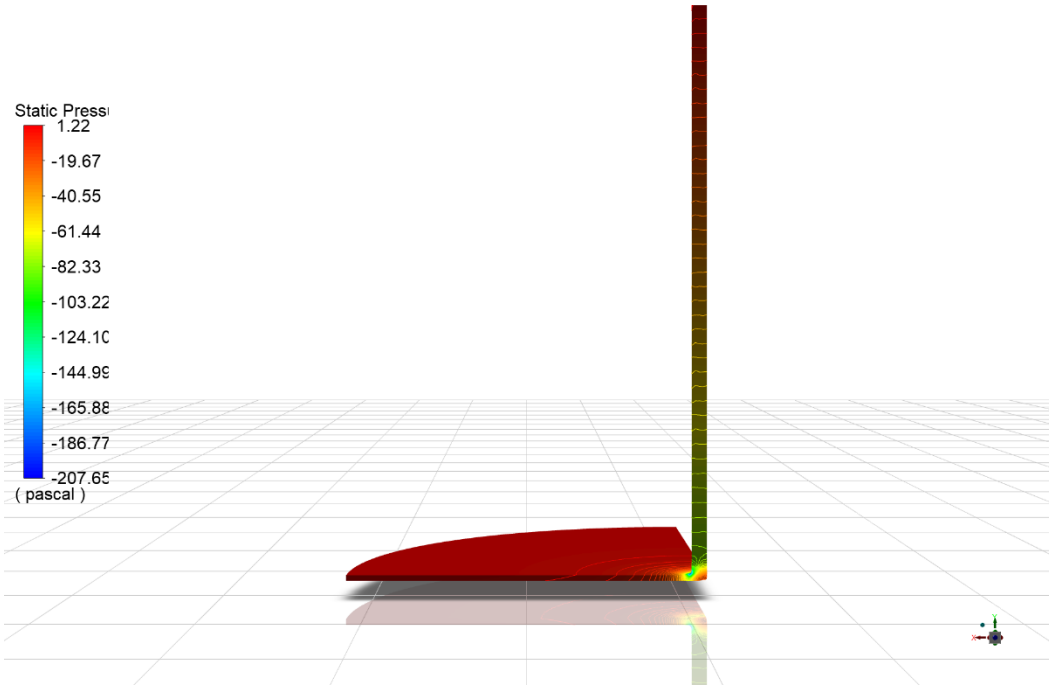

Figure 3.7. Pressure distribution in SCPP.

Table 3.1 gives the simulation findings. According to all of the previous figures of temperature, pressure, and velocity the important part is the chimney base (tower nick)

where the velocity is maximum and the pressure is minimum which is the most suitable place to install the turbine. Also, the temperature is maximum at the absorber.

Table 3.1. Simulation findings.

η	1.27214%	$\dot{W}_t$ [W]	532413	$\dot{Q}_{solar}$ [W]	4.18516e+07
Nu	12220.4	Ra	1.79107e+14	Gr	2.46276e+14
L_c [m]	57.71	β [1/K]	0.00314032	ν [m^2/s]	1.59709e-05

3.2. FINED COLLECTOR SURFACE

The fins idea comes to the picture to increase the plant's gain heat with minimizing the overall size of the plant especially in the collector part. For a better explanation, the following figures are provided for temperature, pressure and velocity.

Figure 3.8 conducts the temperature distribution in the entire body and how the adjacent areas next to the fins are affected. The fins enhance the temperature distribution along with the airflow, unlike the traditional model where the air temperature increases gradually i.e. The air is directly heated up, unlike the conventional model. For a better view and clarification Figure 3.9 and Figure 3.10, which are taken without boundary values just to show the temperature behavior in the arrangement (the side legend is taken without boundaries values), are used.

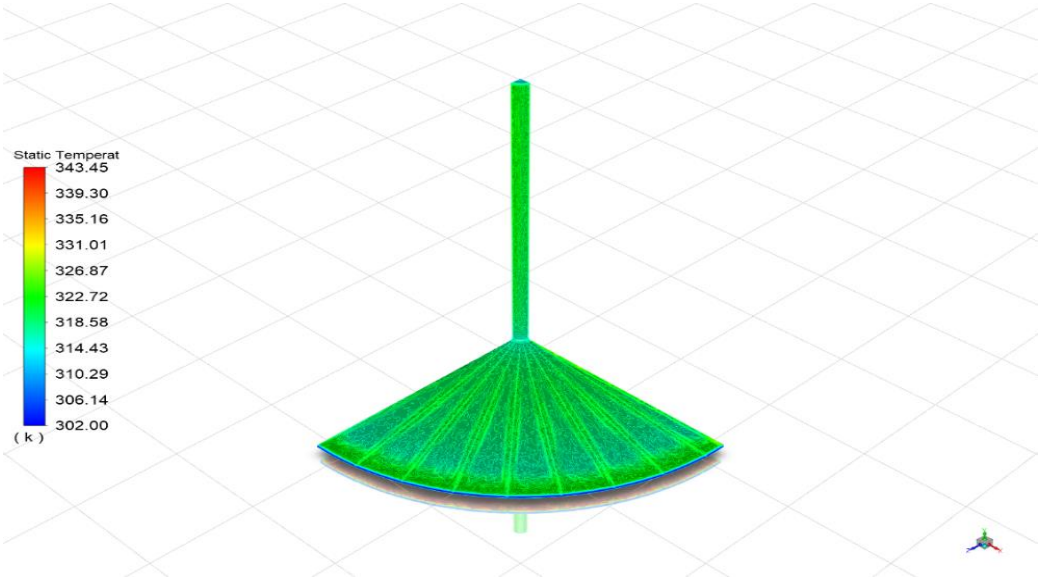

Figure 3.8. Temperature distribution in finned collector surface.

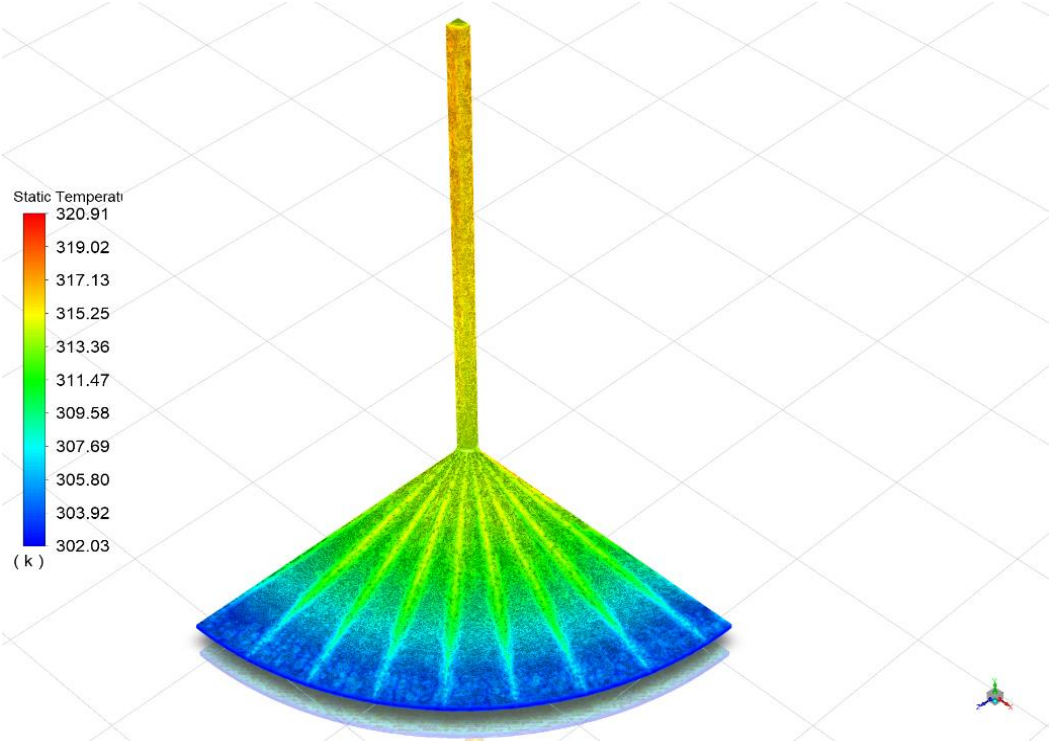

Figure 3.9. Temperature distribution in finned collector surface without boundaries.

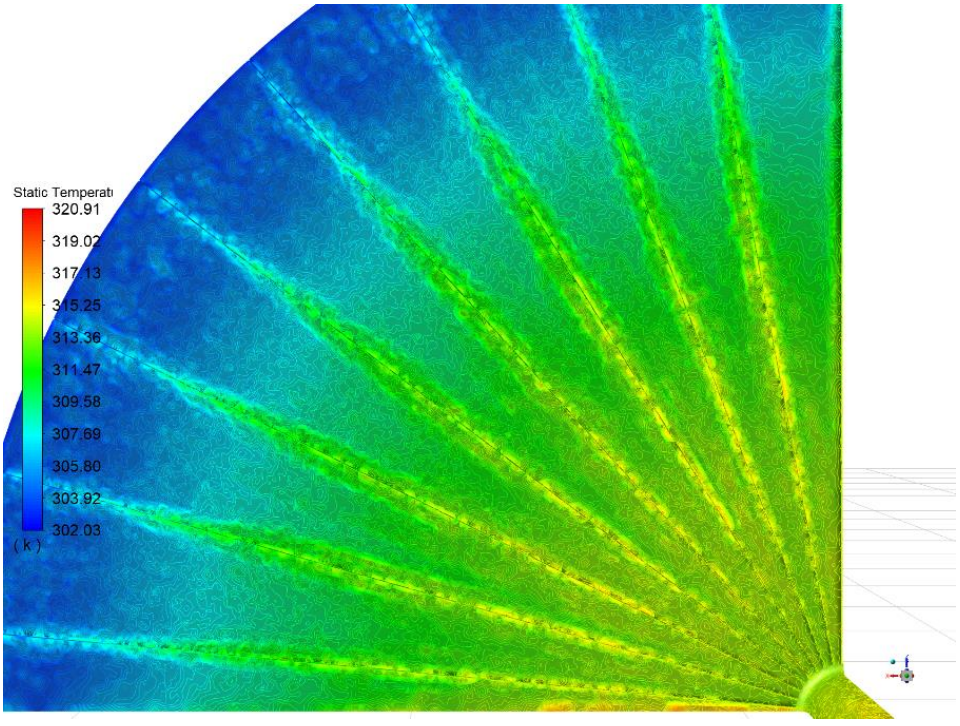

Figure 3.10. Temperature distribution in finned collector surface (detail view).

Figure 3.11 and Figure 3.12 provide the velocity vector of the plant. The air in here acts like the simulated prototype where the velocity increases slowly until reaching the chimney base then slows down again until the outlet. The darkest blue region in Figure 3.11 like lines present fins where the air movement is stationary. By comparing these figures with the traditional simulation (Figure 3.1), it's noticeable that the fin system decreases the velocity a little bit because of the places which are taken by the fins i.e. The mass flow rate becomes less because of flow running areas, and the flow carries more energy.

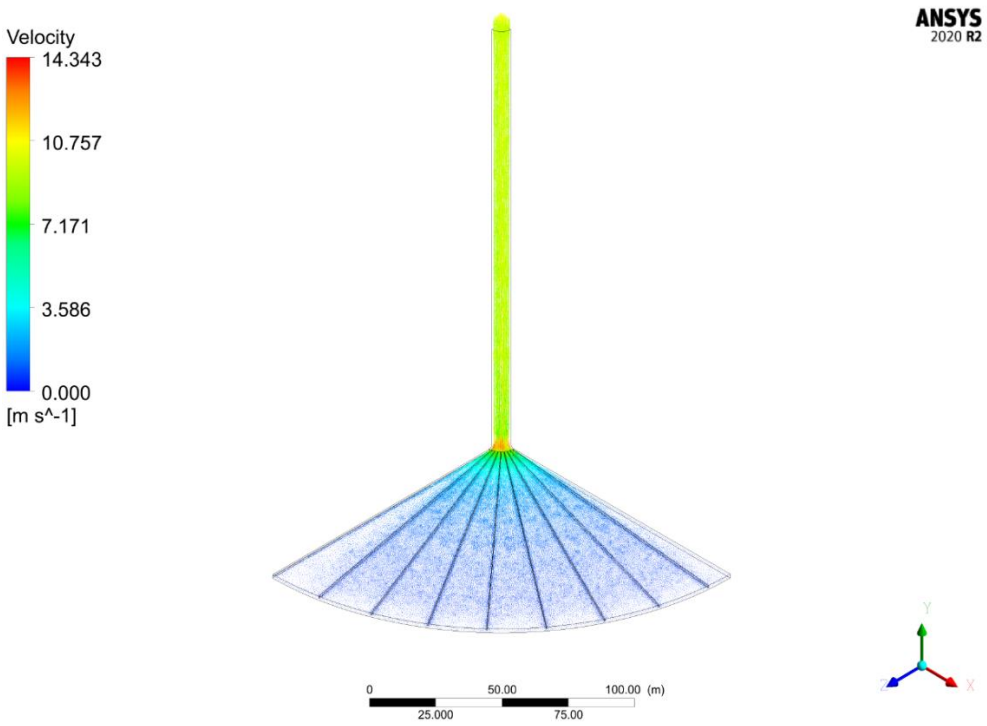

Figure 3.11.Velocity vector distribution in finned collector surface.

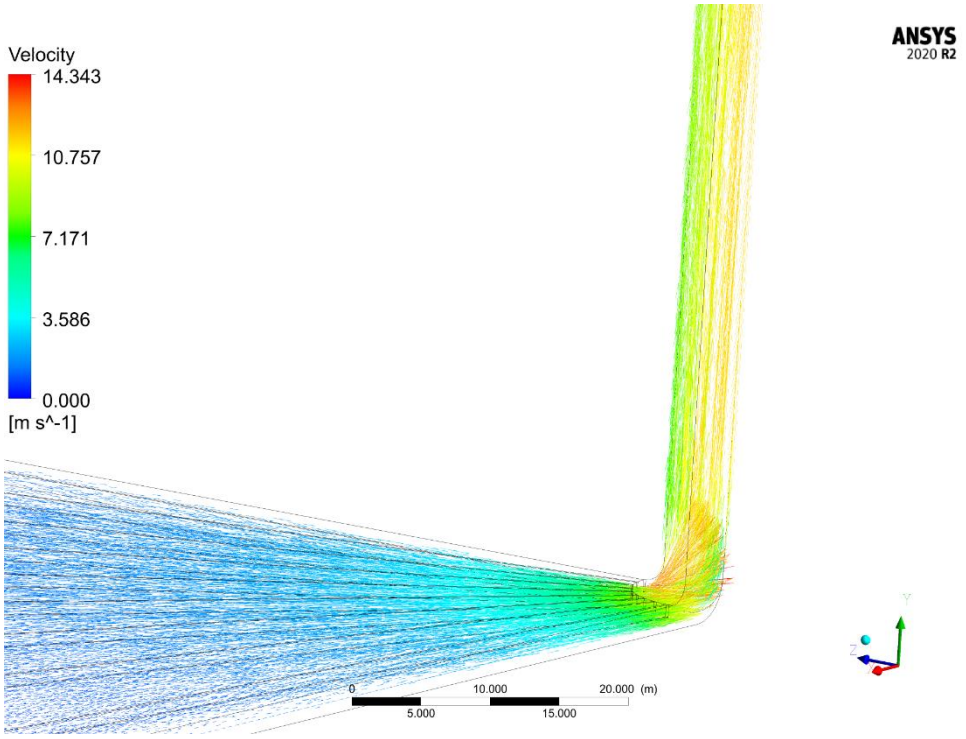

Figure 3.12. Velocity vector distribution on tower base.

Figure 3.13 and Figure 3.14 explain the pressure counters. The pressure acts like the non-fined surface with a small increase in its amount because of decreasing the generated velocity within the system.

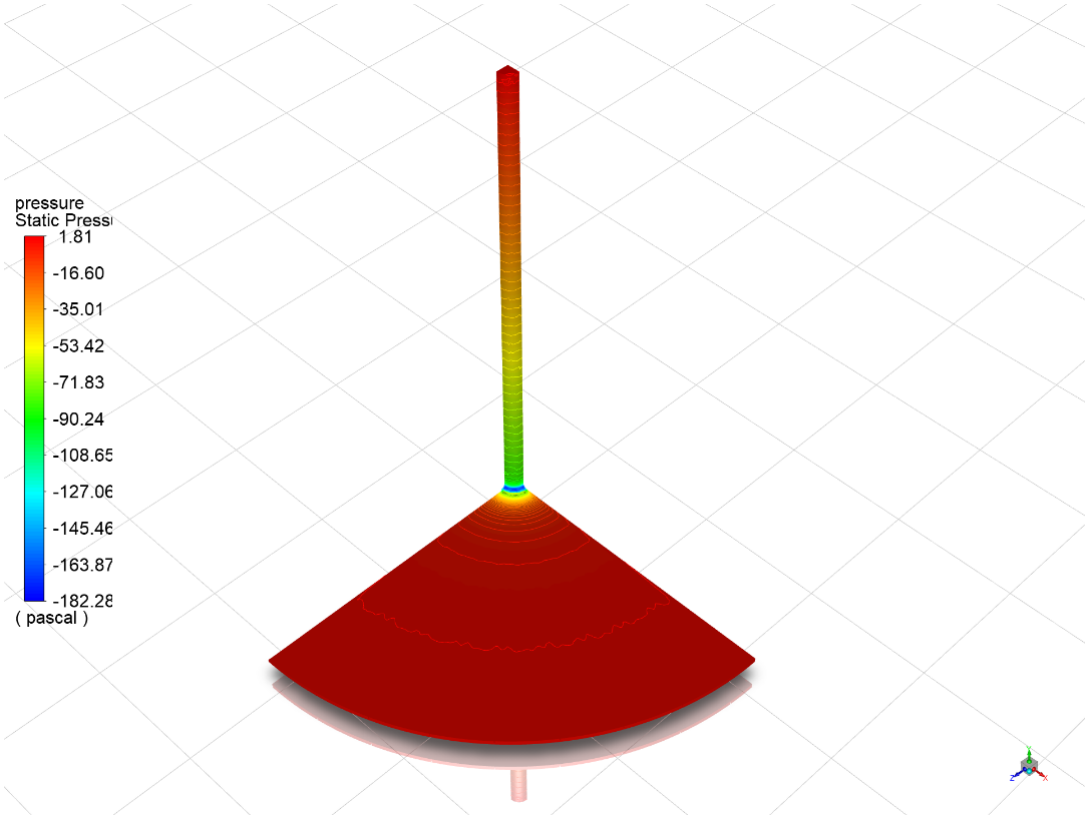

Figure 3.13. Pressure distribution in finned collector surface.

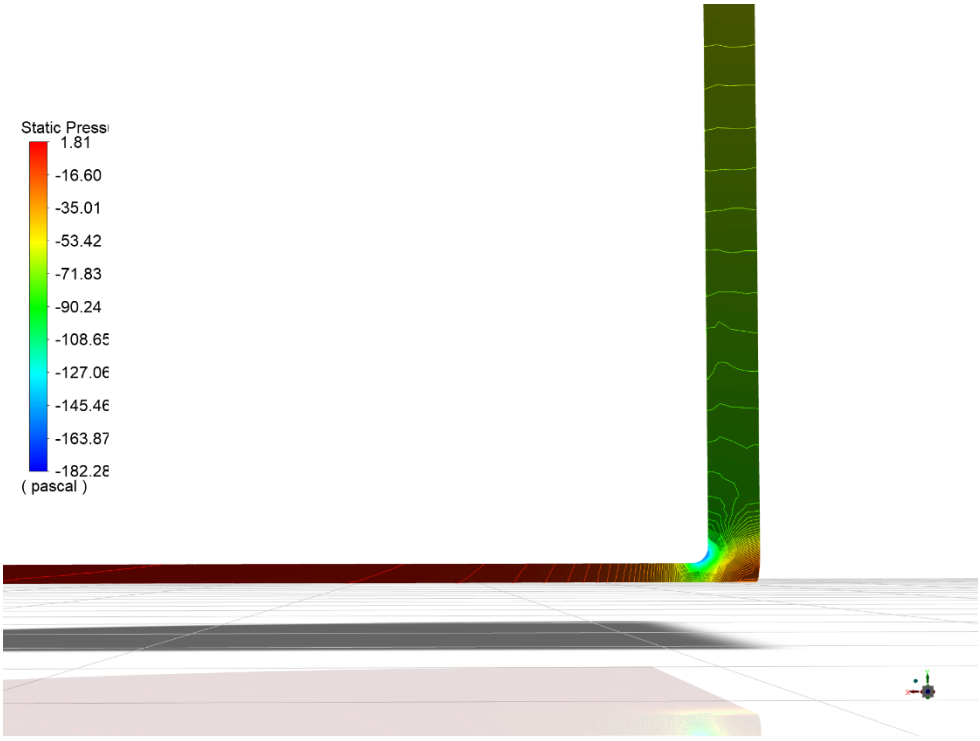

Figure 3.14. Pressure distribution on the chimney base.

Table 3.2 gives the simulation findings of the *SCPP* with finned collector surface. By comparing Table 3.2, which describes the fins features, with Table 3.1. It's found that the system is more stable i.e. ΔT_{mean} is much closer from experimental data than the one without fins. Same as temperature and velocity, while there is a noticeable increase in *Ra* and *Gr* which indicate a better turbulent flow within the system and a decrease in *Nu* indicating a lower convection heat transfer regarding conduction heat transfer all of that leads to a better energy quality i.e. A higher collecter surface area or heat flux will get more power, this concept is visualized clearly by comparing both systems' efficiencies and power outputs. To get a better understanding and to validate the idea a parametric study has been carried out.

Table 3.2. Simulation findings of the *SCPP* with finned collector surface.

η	1.29694%	$\dot{W}_t$ [W]	542790	$\dot{Q}_{solar}$ [W]	4.18516e+07
Nu	4510.33	**Ra**	2.0073e+14	**Gr**	2.76008e+14
Lc [m]	57.71	**β [1/K]**	0.00312918	**ν [m²/s]**	1.59709e-05
ΔT_{mean}	20.725	**T [K]**	343.45	**V [m/s]**	14.45

3.3. PARAMETRIC STUDIES

This section discusses the changes on the fined plant to evaluate the solution and obtain the optimum fin characters.

3.3.1. Variation of Fin Number

Figure 3.15 gives variation of efficiency of the *SCPP* with *Ra* for different fin numbers. It's obtained that the increment in *Ra* increases the efficiency by having too many fins. However, the enlarge in *Ra* will decrease the efficiency by having fewer fins. I.e., by marking fin number of 25, which present the few fins' numbers, the efficiency decreases rapidly with an increase in the turbulent motion then it's getting better when adding more fins, the decrease becomes gradually of fin number of 33, later on, the entire system acts oppositely where the efficiency improving with raising the fluid motion with fin number of 46. All of that leads to choose 46.

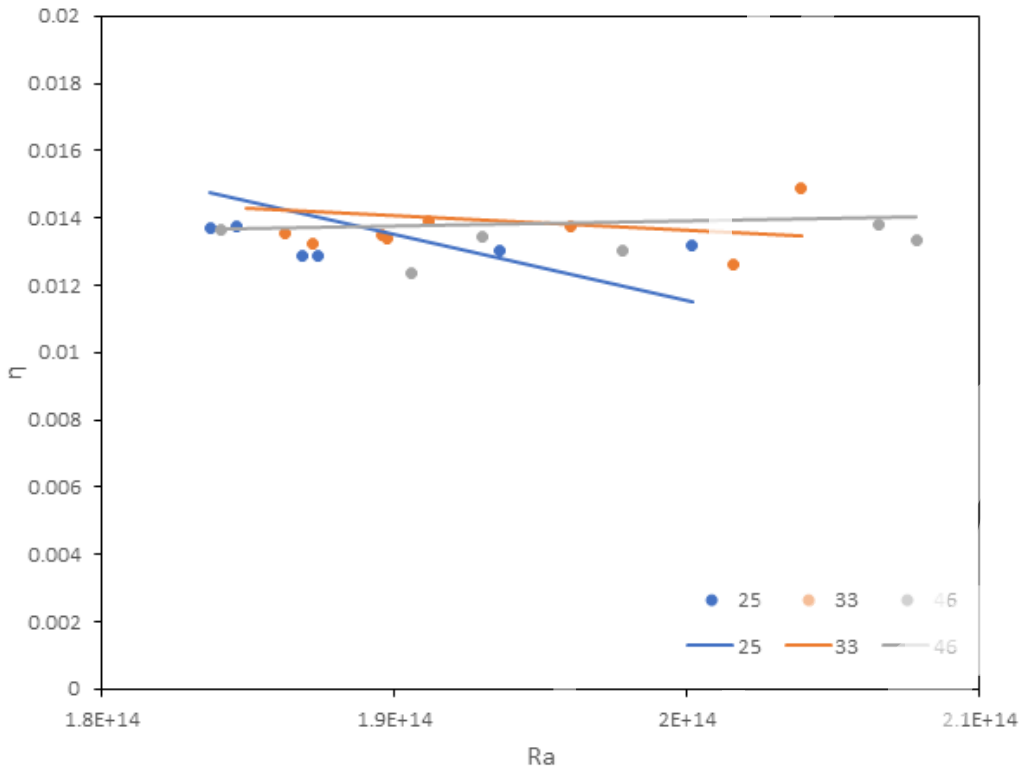

Figure 3.15. Variation of η with Ra for different fins numbers.

Figure 3.16 indicates variation of *Nu* with *Ra* for different fin numbers. It is found that increasing *Ra* decreases *Nu* gradually. Also, adding more fins gives the negative effect on the convective heat transfer rate (conduction heat transfer increases). In total, this condition can satisfy the idea that the entire plant can be minimized with the same amount of heat by rising fins' numbers. I.e., by taking a look at fin number of 46 case, it has the highest efficiency with the lowest *Nu* which serves the goal very well (high efficiency and small plant size) unlike 25 where improving in *Nu* comes on the account of dropping the station efficiency. Hence, from the information of the Figure 3.15 and Figure 3.16, the case of fin number of 46 can be defined as the best fin number for this study.

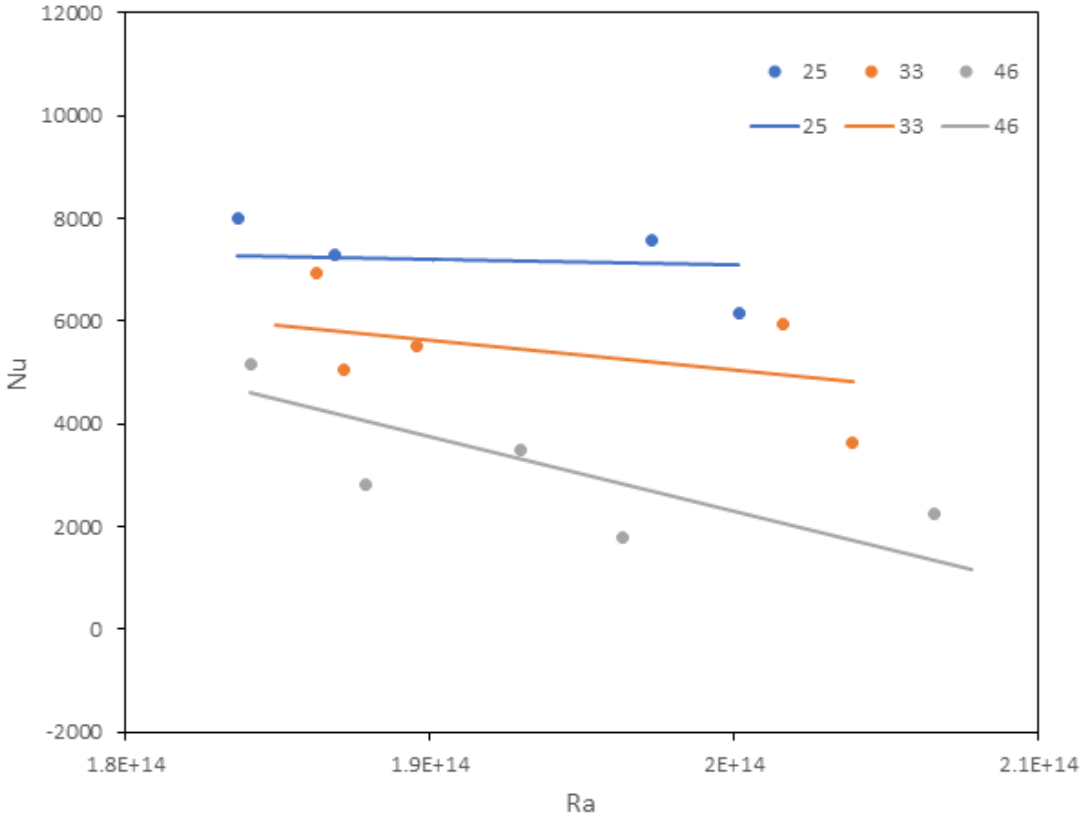

Figure 3.16. Variation of *Nu* with *Ra* for different fin numbers.

3.3.2. Variation of Fins Thickness

Variation of system efficiency with *Ra* for different fin thickness is presented in Figure 3.17. Depending on Figure 3.17 the efficiency tends to be greater with small thickness and to be worse with large thickness even with increasing *Ra*. The reason behind that is the mass flow rate where it becomes more with tiny thickness due to small spaces that fins use them in the flow direction, unlike bigger thickness which gets more spaces so less amount of fluid flow. For the same reason, the fluid has enough space to run into chaotically and vice versa for thicker fins.

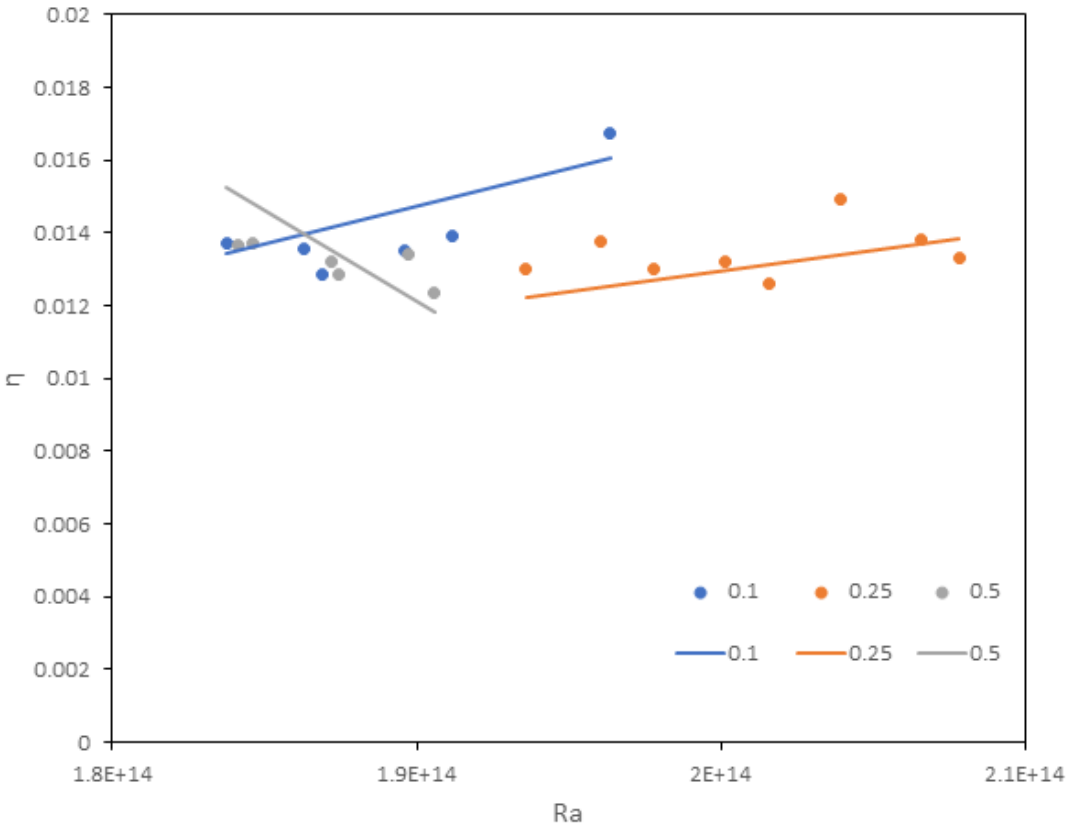

Figure 3.17. Variation of η with *Ra* for different fin thickness.

Figure 5.18 gives the variation of *Nu* with *Ra* for different fin thickness. The data tend to decrease *Nu* with increasing *Ra* for all cases. The decrease for all thicknesses is rapid but it tends to be less curser for small thickness (it can resist the flow motion type for better convection heat transfer) because of the amount of mass flow rate and huger spaces between fins. In the light of Figure 5.17 and Figure 5.18, fin thickness of 0.1 is chosen to be the best thickness of this study.

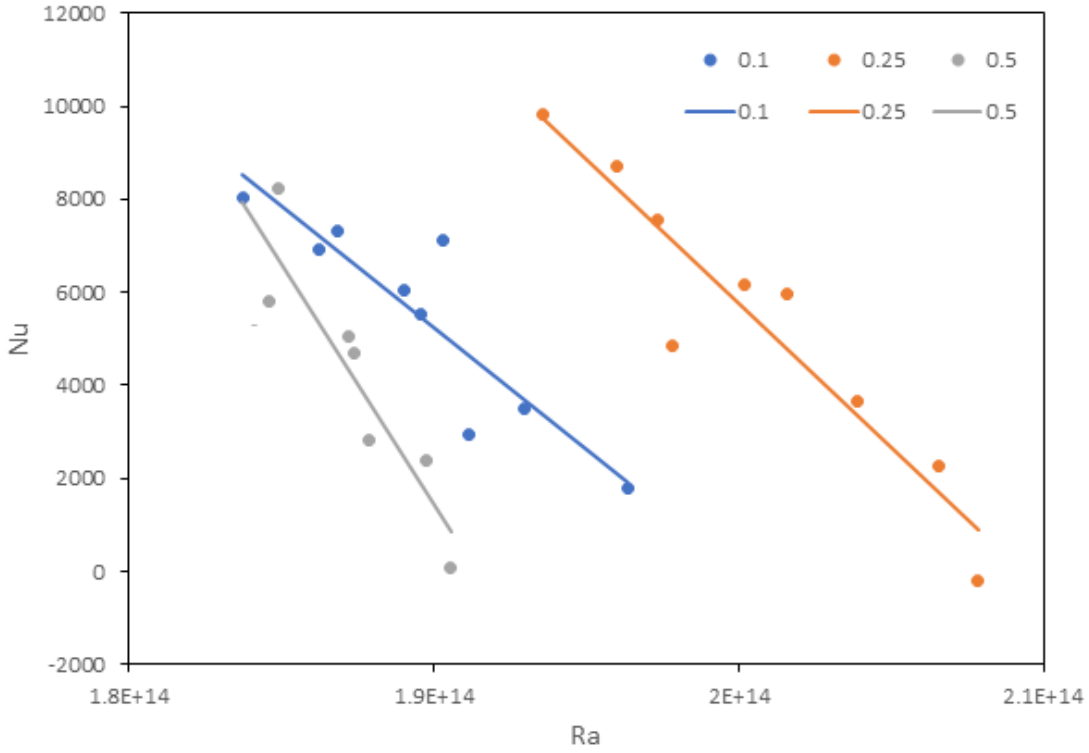

Figure 3.18. Variation of *Nu* with *Ra* for different fin thickness.

3.3.3. Variation of Fins Tallness

Figure 3.19 shows the variation of efficiency of the system with *Ra* for different fin tallness. It's obtained that the case of the fin tallness of 1.2 *m* has the highest impact on the efficiency. This effect drops for other heights because of higher interactive areas (the faces of the fins) with flow motion to transfer more heat through.

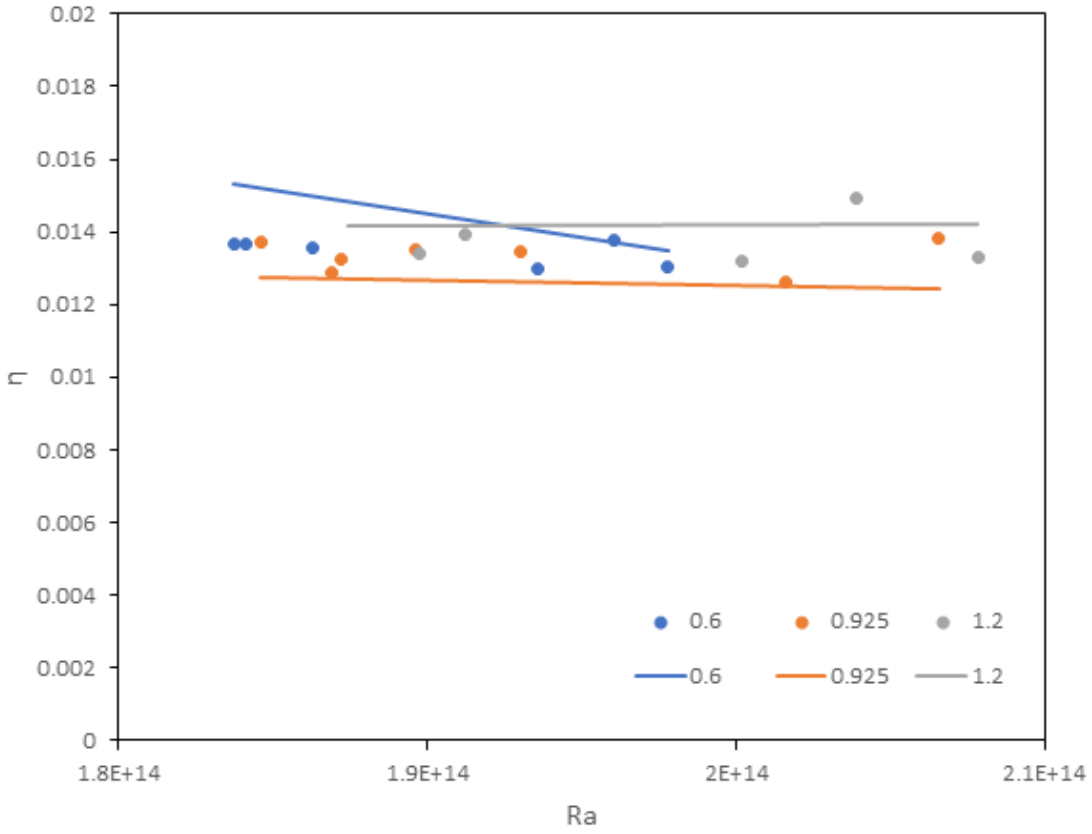

Figure 3.19. Variation of η with *Ra* for different fin tallness.

Figure 3.20 shows the variation of *Nu* with *Ra* for different fin tallness. It is seen in the figure that the shorter fin becomes better for convective heat transfer rate. Otherwise for tall fins but at the same time, this figure serves the same aim again which is a small plant with high efficiency. According to Figure 3.19 and Figure 3.20, 1.2 *m* is selected because it achieves the goal very well.

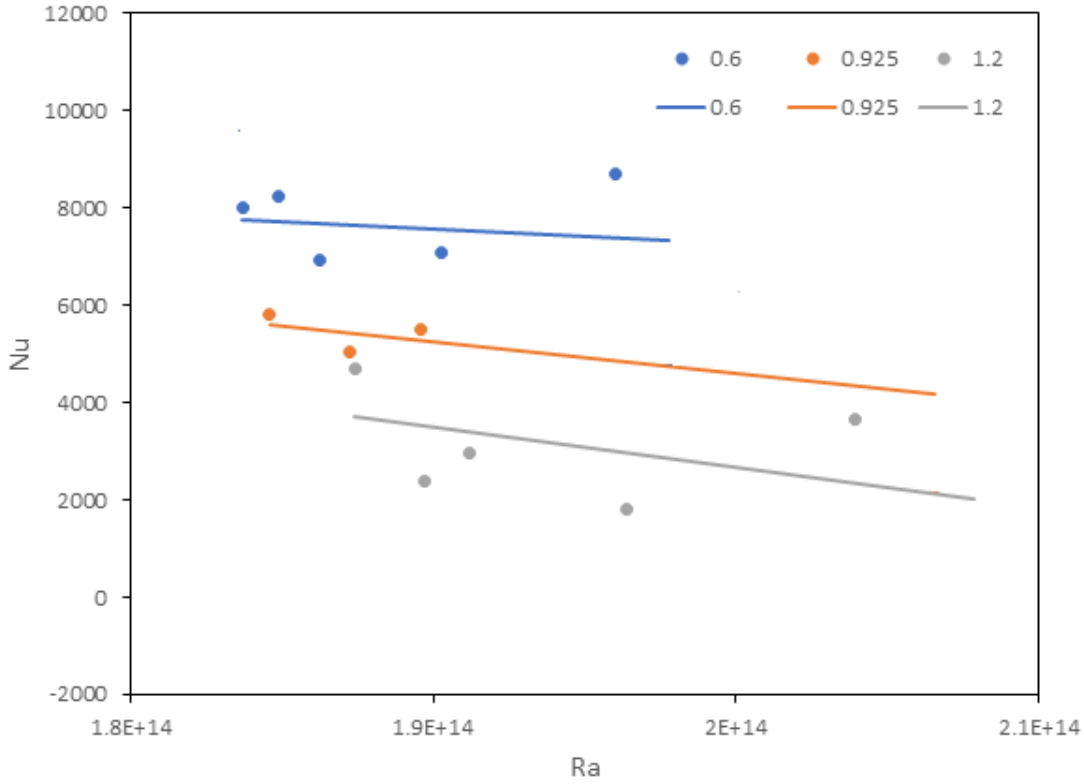

Figure 3.20. Variation of *Nu* with *Ra* for different fin tallness.

3.3.4. Parametric Study Table

Table 3.3 shows all of the numerical calculation results of the study.

Table 3.3. fins parametric study data.

Fin number	***Fin thickness [m]***	***Fin height [m]***	***Ra***	***Gr***	***Nu***	***W_t [W]***	***η***
33	0.25	0.925	2.02E+14	2.77E+14	5943.37	528371	0.012625
33	0.25	0.6	1.96E+14	2.7E+14	8701.09	575475	0.01375
33	0.25	1.2	2.04E+14	2.8E+14	3644.15	624090	0.014912
33	0.1	0.925	1.9E+14	2.61E+14	5507.18	565434	0.01351
33	0.1	0.6	1.86E+14	2.56E+14	6923.34	567491	0.01356
33	0.1	1.2	1.91E+14	2.63E+14	2944.4	582359	0.013915
33	0.5	0.925	1.87E+14	2.57E+14	5060.16	553390	0.013223
33	0.5	0.6	1.85E+14	2.54E+14	8249.63	712138	0.017016
33	0.5	1.2	1.9E+14	2.61E+14	2382.44	560361	0.013389
25	0.25	0.925	1.97E+14	2.71E+14	7567.54	391541	0.009355
25	0.25	0.6	1.94E+14	2.66E+14	9836.62	544424	0.013008
25	0.25	1.2	2E+14	2.75E+14	6170.36	552534	0.013202
25	0.1	0.925	1.87E+14	2.57E+14	7302.14	538573	0.012869
25	0.1	0.6	1.84E+14	2.53E+14	8014.6	572981	0.013691
25	0.1	1.2	1.89E+14	2.6E+14	6029.01	703728	0.016815
25	0.5	0.925	1.85E+14	2.54E+14	5819.55	574924	0.013737
25	0.5	0.6	1.84E+14	2.53E+14	9526.3	700014	0.016726
25	0.5	1.2	1.87E+14	2.58E+14	4707.55	538144	0.012858
46	0.25	0.925	2.07E+14	2.84E+14	2261.46	578200	0.013816
46	0.25	0.6	1.98E+14	2.72E+14	4862.53	545145	0.013026
46	0.25	1.2	2.08E+14	2.86E+14	-189.26	557543	0.013322
46	0.1	0.925	1.93E+14	2.65E+14	3496.08	563478	0.013464
46	0.1	0.6	1.9E+14	2.62E+14	7100.63	720930	0.017226
46	0.1	1.2	1.96E+14	2.7E+14	1790.3	700597	0.01674
46	0.5	0.925	1.88E+14	2.58E+14	2809.04	459744	0.010985
46	0.5	0.6	1.84E+14	2.53E+14	5154.42	570942	0.013642
46	0.5	1.2	1.91E+14	2.62E+14	76.5877	517253	0.012359

3.3.5. Optimum Fin Dimension

Counting on the previous discussion of varying fin parameters (number, thickness, and height), the optimum fin parameters have been selected and given Table 3.4.

Table 3.4. Optimum fin parameters.

Fin number	***Fin thickness [m]***	***Fin height [m]***	***Ra***	***Gr***	***Nu***	***W_t [W]***	***η***
46	0.1	1.2	1.96E+14	2.7E+14	1790.3	700597	1.674%

3.3.6. Comparison of the Calculation Results of the Scpp with Fins and Without Fins

Table 3.5 gives the numerical results for the plain and finned collector. It can be obtained that adding fin on the collector surface increases efficiency and decrease the convective heat transfer rate on the surface. These findings are also in harmony with literature [27,44,45]

Table 3.5. Comparison of the numerical results for plain and finned collector surfaces of the *SCPP*.

	η	***Nu***	***Ra***
Plain Collector	1.27214%	12220.4	1.79107e+14
Finned Collector	1.674%	1790.3	1.96E+14

PART 4

CONCLUSION AND FUTURE WORK

4.1. CONCLUSIONS

Solar chimney power plant *SCPP* is one of the promising technologies for several decades because of its naivety, low material, and maintenance cost, long operating period. It is also whole-round player namely works day and night with any weather condition, in contrast, the system has some problems like low plant efficiency and big plant size for that a farther enhancement is required where in this paper a performance optimization by using fined collector surface is applied. A *3D*-model is presented by utilizing Ansys 2020R2 with Standard *k-ε* model turbulence and *DO* model for solar calculations. The numerical findings are compared with the Spanish prototype to get more realistic results afterward the proposed method is applied and parametrized to get the following conclusions:

- Too many fins show better efficiency and worse *Nu* because of decreasing in convection heat transfer rate on the collector surface.
- Thinner fins give more mass flow rate runs into the system which boosts the efficiency.
- Taller fins mean more interactive areas with flow motion to transfer heat leading to better efficiency.

For that the optimum and the most suitable fin parameters are 46, 0.1 *m*, 1.2 *m* which are the number of fins, fin thickness, and fin height, respectively. This case gives 1.674%, 700597 W, 1790.3, and 1.96E+14 as a plant efficiency, plant power outcome, Nusselt number, and Rayleigh number, respectively where the outcomes of that ideal fin aren’t the highest but it does a good turn to achieve the main purpose of this study

(small plant dimension or huger collecting area and high efficiency) regarding that the natural convection is enhanced by decreasing it.

4.2. SUGGESTIONS FOR FUTURE WORK

- Having a real experiment with new materials is a good idea to verify the work very well because all investigations count on the Manzanares pilot which is too old, especially a large scale one set it up in local a region.
- Fin method could be a very good assistant for collector adjustments especially the inclined, which is the most promising way to get high efficiency, because it eliminates the secondary flow problem of that type.
- While building a plant, the plant should have inclinations in its collector and chimney for better power generation.
- *SCPP* is a promising technology when it's hybridized with other sources for example it could be used with a shallow geothermal resource or/with different heat storage, etc.
- Up until now few studies conducted the chimney issue for that a novel tower or new ways should be invented to minimize the tower height.
- When building a pilot, the new methods should be considered.

REFERENCES

1. Cengel, Y. A. and Ghajar, A. J., "Heat and Mass Transfer: Fundamentals and Applications", 5. Ed., ***McGraw-Hill Professional***, New York, NY, (2014).

2. Haaf, W., Friedrich, K., Mayr, G., and Schlaich, J., "Solar Chimneys Part I: Principle and Construction of the Pilot Plant in Manzanares", ***International Journal Of Solar Energy***, 2 (1): 3–20 (1983).

3. Haaf, W., "Solar Chimneys: Part II: Preliminary Test Results from the Manzanares Pilot Plant", ***International Journal Of Solar Energy***, 2 (2): 141–161 (1984).

4. "Solar Chimney Power Plant Generating Technology - 1st Edition", **https://www.elsevier.com/books/solar-chimney-power-plant-generating-technology/ming/978-0-12-805370-6** (2022).

5. Cuce, E., Cuce, P. M., and Sen, H., "A thorough performance assessment of solar chimney power plants: Case study for Manzanares", ***Cleaner Engineering And Technology***, 1: 100026 (2020).

6. Guo, P., Li, T., Xu, B., Xu, X., and Li, J., "Questions and current understanding about solar chimney power plant: A review", ***Energy Conversion And Management***, 182: 21–33 (2019).

7. Ming, T., "Solar Chimney Power Plant Generating Technology", Solar Chimney Power Plant Generating Technology, (2016).

8. Cottam, P. J., Duffour, P., Lindstrand, P., and Fromme, P., "Solar chimney power plants – Dimension matching for optimum performance", ***Energy Conversion And Management***, 194: 112–123 (2019).

9. Yapıcı, E. Ö., Ayli, E., and Nsaif, O., "Numerical investigation on the performance of a small scale solar chimney power plant for different geometrical parameters", ***Journal Of Cleaner Production***, 276: 122908 (2020).

10. Ghalamchi, M., Kasaeian, A., Ghalamchi, M., and Mirzahosseini, A. H., "An experimental study on the thermal performance of a solar chimney with different dimensional parameters", ***Renewable Energy***, 91: 477–483 (2016).

11. Mehdipour, R., Golzardi, S., and Baniamerian, Z., "Experimental justification of poor thermal and flow performance of solar chimney by an innovative indoor experimental setup", ***Renewable Energy***, 157: 1089–1101 (2020).

12. Eryener, D., Hollick, J., and Kuscu, H., "Thermal performance of a transpired solar collector updraft tower", ***Energy Conversion And Management***, 142: 286–295 (2017).

13. Mehdipour, R., Baniamerian, Z., Golzardi, S., and Murshed, S. M. S., "Geometry modification of solar collector to improve performance of solar chimneys", ***Renewable Energy***, 162: 160–170 (2020).

14. Khidhir, D. K. and Atrooshi, S. A., "Investigation of thermal concentration effect in a modified solar chimney", ***Solar Energy***, 206: 799–815 (2020).

15. Avcı, A. S., Karakaya, H., and Durmuş, A., "Numerical and experimental investigation of solar chimney power plant system performance", ***Energy Sources, Part A: Recovery, Utilization, And Environmental Effects***, 1–19 (2020).

16. Nasraoui, H., Driss, Z., Ayadi, A., Bouabidi, A., and Kchaou, H., "Numerical and experimental study of the impact of conical chimney angle on the thermodynamic characteristics of a solar chimney power plant", ***Proceedings Of The Institution Of Mechanical Engineers, Part E: Journal Of Process Mechanical Engineering***, 233 (5): 1185–1199 (2019).

17. Belkhode, P., Sakhale, C., and Bejalwar, A., "Evaluation of the experimental data to determine the performance of a solar chimney power plant", ***Materials Today: Proceedings***, 27: 102–106 (2020).

18. Ayadi, A., Bouabidi, A., Driss, Z., and Abid, M. S., "Experimental and numerical analysis of the collector roof height effect on the solar chimney performance", ***Renewable Energy***, 115: 649–662 (2018).

19. RahimiLarki, M., Abardeh, R. H., Rahimzadeh, H., and Sarlak, H., "Performance analysis of a laboratory-scale tilted solar chimney system exposed to ambient crosswind", ***Renewable Energy***, 164: 1156–1170 (2021).

20. Mokrani, O. B. E. K., Ouahrani, M. R., Sellami, M. H., and Segni, L., "Experimental investigations of hybrid: geothermal water/solar chimney power plant", ***Energy Sources, Part A: Recovery, Utilization, And Environmental Effects***, 1–18 (2020).

21. Huang, M.-H., Chen, L., Lei, L., He, P., Cao, J.-J., He, Y.-L., Feng, Z.-P., and Tao, W.-Q., "Experimental and numerical studies for applying hybrid solar chimney and photovoltaic system to the solar-assisted air cleaning system", ***Applied Energy***, 269: 115150 (2020).

22. Sangi, R., Amidpour, M., and Hosseinizadeh, B., "Modeling and numerical simulation of solar chimney power plants", ***Solar Energy***, 85 (5): 829–838 (2011).

23. Babin, T., Ramanathan, S., Muthukumar, S., Arun, A. P., and Subbiah, S., "Numerical investigation of backflow in natural draft chimneys", ***Materials Today: Proceedings***, 45: 1196–1204 (2021).

24. Abdelmohimen, M. A. H. and Algarni, S. A., "Numerical investigation of solar chimney power plants performance for Saudi Arabia weather conditions", ***Sustainable Cities And Society***, 38: 1–8 (2018).

25. Cuce, E., Sen, H., and Cuce, P. M., "Numerical performance modelling of solar chimney power plants: Influence of chimney height for a pilot plant in Manzanares, Spain", ***Sustainable Energy Technologies And Assessments***, 39: 100704 (2020).

26. Kebabsa, H., Said Lounici, M., and Daimallah, A., "Numerical investigation of a novel tower solar chimney concept", ***Energy***, 214: 119048 (2021).

27. Das, P. and Chandramohan, V. P., "3D numerical study on estimating flow and performance parameters of solar updraft tower (SUT) plant: Impact of divergent angle of chimney, ambient temperature, solar flux and turbine efficiency", ***Journal Of Cleaner Production***, 256: 120353 (2020).

28. Keshari, S. R., V.P., C., and Das, P., "A 3D numerical study to evaluate optimum collector inclination angle of Manzanares solar updraft tower power plant", ***Solar Energy***, 226: 455–467 (2021).

29. Kebabsa, H., Lounici, M. S., Lebbi, M., and Daimallah, A., "Thermo-hydrodynamic behavior of an innovative solar chimney", ***Renewable Energy***, 145: 2074–2090 (2020).

30. Hassan, A., Ali, M., and Waqas, A., "Numerical investigation on performance of solar chimney power plant by varying collector slope and chimney diverging angle", ***Energy***, 142: 411–425 (2018).

31. Kasaeian, A., Mahmoudi, A. R., Astaraei, F. R., and Hejab, A., "3D simulation of solar chimney power plant considering turbine blades", ***Energy Conversion And Management***, 147: 55–65 (2017).

32. Zuo, L., Qu, N., Liu, Z., Ding, L., Dai, P., Xu, B., and Yuan, Y., "Performance study and economic analysis of wind supercharged solar chimney power plant", ***Renewable Energy***, 156: 837–850 (2020).

33. Pratap Singh, A., Kumar, A., Akshayveer, and Singh, O. P., "Performance enhancement strategies of a hybrid solar chimney power plant integrated with photovoltaic panel", ***Energy Conversion And Management***, 218: 113020 (2020).

34. Kashiwa, B. A. and Kashiwa, C. B., "The solar cyclone: A solar chimney for harvesting atmospheric water", ***Energy***, 33 (2): 331–339 (2008).

35. Zuo, L., Dai, P., Liu, Z., Qu, N., Ding, L., Qu, B., and Yuan, Y., "Numerical analysis of wind supercharging solar chimney power plant combined with seawater desalination and gas waste heat", ***Energy Conversion And Management***, 223: 113250 (2020).

36. Abdelsalam, E., Kafiah, F., Tawalbeh, M., Almomani, F., Azzam, A., Alzoubi, I., and Alkasrawi, M., "Performance analysis of hybrid solar chimney–power plant for power production and seawater desalination: A sustainable approach", ***International Journal Of Energy Research***, 45 (12): 17327–17341 (2021).

37. Sedighi, A. A., Deldoost, Z., and Karambasti, B. M., "Effect of thermal energy storage layer porosity on performance of solar chimney power plant considering turbine pressure drop", ***Energy***, 194: 116859 (2020).

38. Attig-Bahar, F., Sahraoui, M., Guellouz, M. S., and Kaddeche, S., "Effect of the ground heat storage on solar chimney power plant performance in the South of Tunisia: Case of Tozeur", ***Solar Energy***, 193: 545–555 (2019).

39. Amudam, Y. and Chandramohan, V. P., "Influence of thermal energy storage system on flow and performance parameters of solar updraft tower power plant: A three dimensional numerical analysis", ***Journal Of Cleaner Production***, 207: 136–152 (2019).

40. Rashidi, S., Esfahani, J. A., and Hosseinirad, E., "Assessment of solar chimney combined with phase change materials", ***Journal Of The Taiwan Institute Of Chemical Engineers***, 124: 341–350 (2021).

41. Omara, A. A. M., Mohammed, H. A., al Rikabi, I. J., Abuelnour, M. A., and Abuelnuor, A. A. A., "Performance improvement of solar chimneys using phase change materials: A review", ***Solar Energy***, 228: 68–88 (2021).

42. Méndez, C. and Bicer, Y., "Comparison of the influence of solid and phase change materials as a thermal storage medium on the performance of a solar chimney", ***Energy Sci Eng***, 9 (8): 1274–1288 (2021).

43. Ashouri, M. and Hakkaki-Fard, A., "Improving the performance of the finned absorber inclined rooftop solar chimney combined with composite PCM and PV module", ***Solar Energy***, 228: 562–574 (2021).

44. Hosseini, S. S., Ramiar, A., and Ranjbar, A. A., "Numerical investigation of rectangular fin geometry effect on solar chimney", ***Energy And Buildings***, 155: 296–307 (2017).

45. Balijepalli, R., Chandramohan, V. P., and Kirankumar, K., "Development of a small scale plant for a solar chimney power plant (SCPP): A detailed fabrication procedure, experiments and performance parameters evaluation", ***Renewable Energy***, 148: 247–260 (2020).

46. Balijepalli, R., Chandramohan, V. P., and Kirankumar, K., "Performance parameter evaluation, materials selection, solar radiation with energy losses, energy storage and turbine design procedure for a pilot scale solar updraft tower", ***Energy Conversion And Management***, 150: 451–462 (2017).

47. Kasaeian, A. B., Molana, S., Rahmani, K., and Wen, D., "A review on solar chimney systems", ***Renewable And Sustainable Energy Reviews***, 67: 954–987 (2017).

48. Cengel, Y. A. and Cimbala, J. M., "Fluid Mechanics Fundamentals and Applications", 3. Ed., ***McGraw-Hill Professional***, New York, NY, (2013).

RESUME

IBRAHIM SHIKH HASAN was born in Aleppo Syria and he graduated from high school in Saudi Arabia. He entered Karabük University in 2014 as a bachelor degree student in the mechanical engineering department and graduated from it in 2018 with a 3.1 GPA. He joined the master's degree in Karabük University in 2018.